Research Paper
Computational Methods for Differential Equations
http://cmde.tabrizu.ac.ir
Vol. 14, No. 1, 2026, pp. 470-501
DOI:10.22034/cmde.2025.67008.3176

A new delayed SEIR-SEI model for dengue transmission control with sensitivity and competitive mathematical analysis

Shah Zeb[1], Siti Ainor Mohd Yatim[1,2,*], Ayesha Kamran[3], Rizwana Kausar[4], and Muhammad Rafiq[5]

[1]School of Distance Education, Universiti Sains Malaysia, 11800, USM, Penang, Malaysia.

[2]School of Mathematical Sciences, Universiti Sains Malaysia, 11800, USM, Penang, Malaysia.

[3]Department of Mathematics, University of Management and Technology, CII Johar Town, Lahore, 54770, Punjab, Pakistan.

[4]School of Biological Sciences, Universiti Sains Malaysia, USM, 11800, Penang, Malaysia.

[5]Department of Mathematics, Namal University, 30km Talagang Road, Mianwali, 42250, Pakistan.

Abstract

Dengue fever is a viral illness affecting over 129 nations and more than 50% of the global population, causing approximately 400 million cases annually. This study explores the mathematical formulation and dynamics of dengue transmission using a structured SEIR-SEI (susceptible human, exposed human, infected human, recovered human, susceptible vector, exposed vector, and infected vector) model, focusing on immunological and delay-based control strategies. An existing nonlinear delayed SEIR-SEI epidemic model is extended to evaluate the effectiveness of awareness, mosquito deterrence, and therapeutic interventions. Rather than immediately resorting to pharmacological methods, the model emphasizes analyzing delay factors due to their significant role in disease control. Since reducing mosquito populations can harm ecological balance, this new approach applies delay-based strategies on human-related factors such as hospitalization, awareness, and travel restrictions to safeguard both public health and the environment. The findings show that the reproductive number alone is insufficient to predict outbreak persistence; recruitment patterns and mosquito biting rates play a more pivotal role. We analyze the model's mathematical properties, including the reproduction number, equilibrium points, parameter sensitivity, and both local and global stability. Our results demonstrate that model-based strategies focusing on vector control and human behavior effectively reduce dengue transmission. Additionally, we show that the non-standard finite difference scheme outperforms traditional methods like the fourth-order Runge-Kutta in terms of accuracy, stability, and predictive capability. This study offers valuable insights for public health officials and policymakers in designing sustainable strategies to control endemic dengue transmission and prevent future outbreaks.

Keywords. Dengue, Reproductive number, Global stability, NSFD, Convergence analysis.

2010 Mathematics Subject Classification. 65L05, 34K06, 34K28.

1. Introduction

Historically, dengue outbreaks have been observed in the last few centuries all over the world. The earliest unconfirmed case of the disease emerged at the dawn of seventeenth century, however, it was not officially documented until the mid-eighteenth century across Africa, Asia, and North America. This disease maintains its continuous presence in numerous parts of the world, affecting almost all the countries across regions such as the Eastern Mediterranean [31], America, Africa, Southeast Asia, and the Western Pacific. Dengue has emerged as a major contributor to both illness and death, being the most common disease. Dengue spread globally after the mid-20th century, significantly impacting emerging countries in the Americas, Africa, the Pacific, and the Caribbean [24]. Major outbreaks were documented in Cuba, Brazil, and Venezuela in 1981, 1986, and 1990, respectively [10]. Currently, dengue-related diseases have been reported in more than 100 countries worldwide. The World Health Organization (WHO) has warned that this disease will affect about half of the world's population in the current century [12]. Climate change has facilitated the disease's

Received: 27 April 2025; Accepted: 27 October 2025.
∗ Corresponding author. Email: ainor@usm.my.

expansion into Southern Europe and parts of the United States. The disease continues to cause both mortality and morbidity, particularly in Southeast Asia, the Caribbean, and Latin America.

In eastern countries like Malaysia, dengue fever was first reported after an outbreak in Penang around December 1901. Since then, dengue incidences have steadily increased and become a significant public health concern [8]. In the last 5 years, dengue cases have continuously risen annually and have been recognized as a major public health problem. Malaysia has been experiencing a surge in the number of dengue cases within the past decade. For instance, the number has increased more than two-fold from 43,346 cases in 2013 to 111,285 cases in 2015 [2]. According to the WHO, Malaysia reported 120,836 dengue cases in 2015, with a case fatality rate of 0.2% [42]. However, in 2019, the country experienced a significant increase, recording 130,101 cases, the highest since 2004 [34]. By October 2023, the number of dengue cases had increased by 100.5%, totaling 96,443 cases, compared to 48,109 cases reported in 2022. These figures highlight the substantial public health burden of dengue in one country. In addition, studies have shown that dengue cases in many countries have been under-reported [23].

Dengue is a mosquito-borne tropical disease caused by the dengue virus [35], transmitted through the bite of female Aedes mosquitoes [30]. The virus is arthropod-borne (arbovirus), consisting of four distinct serotypes that do not provide lasting immunity against each other [21]. Infected female Aedes mosquitoes are responsible for the transmission of dengue disease among humans, animals, and even themselves [14]. While Aedes aegypti mosquitoes are the primary vectors, Aedes albopictus mosquitoes also contribute to the transmission, albeit to a lesser extent. Female Aedes mosquitoes become infected when they feed on the blood of a human during the viremic stage of the illness. Once infected, these mosquitoes can transmit the virus to other susceptible humans. Besides, vertical transmission (disease transmission from an infected mother to a child and infected human to another human) is another factor affecting many pathogens, and diseases, including dengue [15]. Recovery from infection with one serotype provides lifelong immunity to that specific serotype but is only capable of providing temporary cross-immunity to the other serotypes [15].

Some initiatives and strategies are available to be implemented on the government-level to curb the spread of dengue. To date, many governments have yet to approve the use of the dengue vaccine [18]. One of the most successful strategies for managing and preventing dengue fever is vector management. The population of Aedes mosquitoes can be decreased by conducting fogging in areas with high dengue cases. However, Aedes mosquitoes have the potential to persist and build resistance to the space spraying chemical, which decreases its efficiency to decrease the spread of dengue [27]. Sprays are overused in different regions and the negative ecological impact of the aerosols from a spray can also be observed on the ozone layer. Another way of controlling the population of Aedes mosquitoes is by utilizing the trap of auto dissemination. This is a proactive approach since the trap includes a specific solution that attracts female Aedes mosquitoes to lay their eggs inside it. The relationship between mosquito population and humans is a complicated phenomenon that is influenced by several variables, including diversity and worldwide climate. Human behaviour is the main factor affecting the handling of these mosquitoes' breeding sites and the decline in their numbers [13]. People who knew more about dengue than people who didn't report using preventative measures at a considerably greater rate. However, contradicting data suggest that information about dengue does not necessarily translate into adopting the advised preventive measures. Previous studies in many countries like Malaysia revealed that most people are generally educated about dengue and ways to prevent it. However, little is known about the relationship between knowledge and dengue preventive behaviours [43]. Therefore, the control program should not solely depend on vector control management. Attention should also be given to the behavioral impact of the people among dengue awareness campaigns. On the other hand, it is also observed that Carica papaya leaf juice has thrombocytosis action in rats and dengue patients. This is a positive development towards the treatment of dengue, however, it requires more scientific research [29].

Dengue presents an enormous economic burden to the government. In Malaysia, it costs approximately 359 million Malaysian ringgits annually [28]. Since dengue has no cure, severe cases require hospitalization and supportive care. Despite various vaccinations demonstrating encouraging trial results, Malaysia has not authorized their use yet. Therefore, dengue can only be controlled by preventing or reducing its transmission. When allocating resources, high-risk areas might be ranked higher than low-risk areas to ensure that effective preventive measures are taken in proportion to the threat posed rather than as a response to an epidemic that has already happened. Thus, it is crucial

to have innovative methods for the early diagnosis of dengue fever, such as using dengue test kits. A cheap, efficient vaccine is essential for universal control. Governments mostly use vector control and insect repellents to lower infection rates. Community education about dengue hazards is essential for prevention. Media campaigns and community involvement may spread preventative knowledge. Community-government miscommunications can raise dengue risk, making ongoing community awareness crucial for successful interventions. Controlling the mosquito vector or preventing human-vector interaction is the only way to stop and manage the dengue virus [39]. Therefore, a trustworthy mathematical model is necessary to provide a more thorough grasp of the dengue transmission process and strategies for halting the disease's spread.

Numerous mathematical models have been developed based on the epidemiology of infectious diseases [7, 16, 44, 45]. These models are typically constructed to understand the interactions between hosts and pathogens and how to control them. By incorporating various factors influencing disease transmission, researchers can analyze their impact on the rise or decline of infection cases. The study of epidemic modeling dates back to 1766 when Daniel Bernoulli formulated a mathematical model to assess the effectiveness of smallpox inoculation [17]. His findings suggested that inoculation could extend life expectancy from birth by approximately three years. Later, Ronald Ross mathematically described malaria transmission dynamics, developing the first malaria model that considered both human and mosquito populations in susceptible and infectious states [25]. His model demonstrated the correlation between mosquito density and malaria incidence in humans. Dengue modeling has been useful in helping us understand the virus's dynamics and in generating some new hypotheses about why the dynamics exhibit certain irregularities, both short-term and long-term. The susceptible–infected–recovered (SIR) model, first proposed by Kermack and McKendrick in 1927, has been widely adopted by researchers to analyze the spread and dynamics of infectious diseases [22]. Compartmental models based on Ordinary Differential Equations (ODEs) are commonly employed to represent vector-host dynamics in the transmission and control of dengue fever.

Recently, there is a rising interest in research focused on mathematical modeling to better understand the spread of dengue epidemics [1, 19, 40]. The escalating incidence of dengue worldwide, with approximately half the global population at risk, underscores the urgency for accurate predictive models that can assist in formulating public health strategies [5]. Nevertheless, the majority of existing research focuses on statistical analyses of dengue incidence [6], literature-based evaluations, or clinical monitoring efforts. While extensive research has been conducted on dengue transmission in eastern countries like Malaysia, the incorporation of delay differential equations (DDEs) into deterministic SEIR-SEI models remain relatively limited. This model refers to the susceptible-exposed-infected-recovered for humans and susceptible-exposed for vectors. Therefore, this study fills that gap by proposing a refined model of vertical transmission that incorporates delay effects that are focused on human dynamics. Given the ecological importance of mosquitoes, controlling their population can disrupt the environmental balance. Hence, this model emphasizes on human-centered delay strategies as a sustainable alternative for understanding and managing disease dynamics. The primary objective of this research is to design a mathematical model to support long-term vector-human coexistence without compromising public health. Some precautions can be applied for human safety. Existing deterministic dengue models [19, 20, 26, 36, 38] were extended by incorporating a time delay parameter resulting in a novel SEIR-SEI model with DDEs. Possible impacts of the biological control strategy on the spread of the disease were investigated and a detailed discussion of sensitive parameters are presented. The stability analysis for both local and global levels were studied under some assumptions on the reproduction number. For the computational analysis, the standard and non-standard finite difference methods were applied to solve the DDEs. The non-standard finite difference method (NSFD) was found to positively preserve the numerical results. In addition, the proposed approach is in a good agreement with the biological properties of the model and independent of the time step size.

This article is structured as follows: A brief history and a review of the literature on dengue are presented in section 1. The formulation of a new model incorporating a time delay factor is discussed in section 2. Then, the equilibrium points, as well as the existence and uniqueness of the new model's solution is covered in section 3. The reproductive number and parameter sensitivity of the reproductive number are presented in section 4, whereas the local and global stability of the system are presented in section 5. The convergence analysis of the NSFD technique and the results of numerical simulations and experiments at different points are showcased in section 6. Lastly, final observations are concluded in section 7.

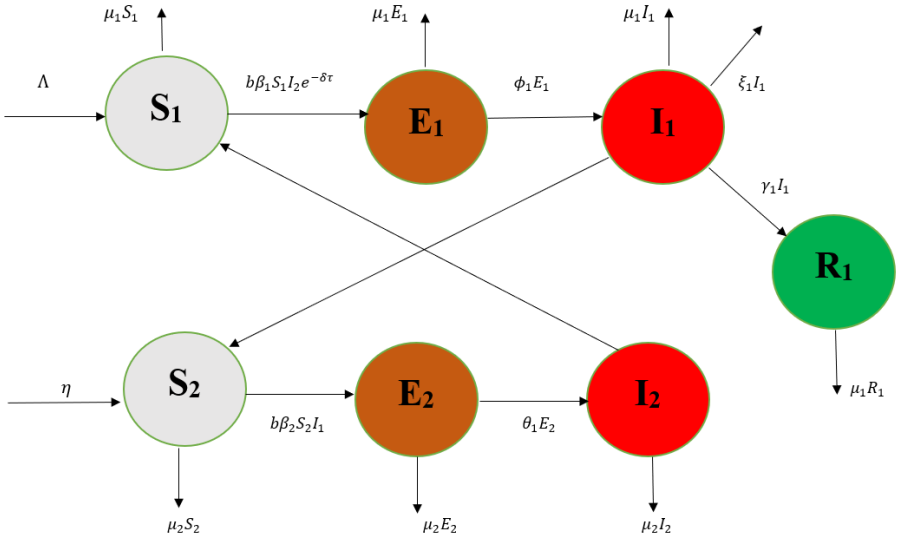

FIGURE 1. Dengue transmission model of human and mosquito populations with delay effects.

2. Delayed SEIR-SEI Model for Dengue Transmission Control

Modeling with DDEs is important in dealing with dangerous diseases like dengue. Implementing delay-based intervention strategies in humans, for instance, has the potential to reduce the spread of dengue. Although the effects may not be immediate, adherence to preventive measures can help limit the transmission of vector-borne diseases. Motivated by this, existing mathematical models are modified by applying time delay measures between susceptible and infected humans. Four compartments representing different human populations are set under the host population $N_1(t)$, namely the susceptible $S_1(t)$, the exposed $E_1(t)$, the infected $I_1(t)$, and the recovered $R_1(t)$. At the same time, three compartments are set under the vector population $N_2(t)$, namely the susceptible S_2, the exposed E_2, and the infected I_2. This setting is converted into the following system and is displayed in Figure 1:

$$N_1 = S_1 + E_1 + I_1 + R_1, \tag{2.1}$$

$$N_2 = S_2 + E_2 + I_2. \tag{2.2}$$

To analyze the transmission dynamics of infectious diseases, various parameters are incorporated into mathematical models. These parameters help quantify factors such as infection rates, recovery rates, and population interactions, providing insights into disease spread and control strategies. Table 1 outlines the key parameters used in this study.

2.1. Model Dynamics and Interactions.

The DDEs that represent the proposed mathematical model are as follows:

$$\frac{dS_1}{dt} = \Lambda - b\beta_1 S_1 I_2 e^{-\delta\tau} - \mu_1 S_1, \tag{2.3a}$$

$$\frac{dE_1}{dt} = b\beta_1 S_1 I_2 e^{-\delta\tau} - (\mu_1 + \phi_1) E_1, \tag{2.3b}$$

$$\frac{dI_1}{dt} = \phi_1 E_1 - (\mu_1 + \gamma_1 + \xi_1) I_1, \tag{2.3c}$$

$$\frac{dR_1}{dt} = \gamma_1 I_1 - \mu_1 R_1, \tag{2.3d}$$

$$\frac{dS_2}{dt} = \eta - b\beta_2 S_2 I_1 - \mu_2 S_2, \tag{2.3e}$$

$$\frac{dE_2}{dt} = b\beta_2 S_2 I_1 - (\theta_2 + \mu_2)E_2, \tag{2.3f}$$

$$\frac{dI_2}{dt} = \theta_2 E_2 - \mu_2 I_2, \tag{2.3g}$$

with starting points

$$S_1(0) > 0, \quad E_1(0) \geq 0, \quad I_1(0) \geq 0, \quad R_1(0) \geq 0, \quad S_2(0) > 0, \quad E_2(0) \geq 0, \quad I_2(0) \geq 0. \tag{2.3h}$$

Here $t \geq 0, \quad \tau \leq t$.

3. Model Analysis

In this segment, a conceptual analysis of the dynamics exhibited by dengue infection is examined. This analysis consists of model properties such as the positivity, boundedness of solution and model equilibrium states.

Theorem 3.1. *The proposed model of disease possesses a non-negative solution, provided non-negative initial conditions for all $t \geq 0$.*

Proof. To prove the solutions' positivity, each equation should be non-negative for non-negative initial conditions. Evaluating each equation at the boundary, where the respective variable is zero yield:

$$\left.\frac{dS_1}{dt}\right|_{S_1=0} = \Lambda - b\beta_1 S_1 I_2 e^{-\delta\tau} - \mu_1 S_1 = \Lambda \geq 0,$$

$$\left.\frac{dE_1}{dt}\right|_{E_1=0} = b\beta_1 S_1 I_2 e^{-\delta\tau} - (\mu_1 + \phi_1)E_1 = b\beta_1 S_1 I_2 e^{-\delta\tau} \geq 0,$$

$$\left.\frac{dI_1}{dt}\right|_{I_1=0} = \phi_1 E_1 - (\mu_1 + \gamma_1 + \xi_1)I_1 = \phi_1 E_1 \geq 0,$$

$$\left.\frac{dR_1}{dt}\right|_{R_1=0} = \gamma_1 I_1 - \mu_1 R_1 = \gamma_1 I_1 \geq 0,$$

$$\left.\frac{dS_2}{dt}\right|_{S_2=0} = \eta - b\beta_2 S_2 I_1 - \mu_2 S_2 = \eta \geq 0,$$

$$\left.\frac{dE_2}{dt}\right|_{E_2=0} = b\beta_2 S_2 I_1 - (\theta_2 + \mu_2)E_2 = b\beta_2 S_2 I_1 \geq 0,$$

Table 1. Descriptions and values of key parameters.

Parameter	Description	Value	Ref
Λ	The recruitment rate of the human or host population	60, 600	[26], EE
η	The recruitment rate of the vector or mosquito population	3000	[26]
μ_1, δ	The natural mortality rate for human population	0.02877	[26]
μ_2	The natural mortality rate for vector population	0.1	[19]
ξ_1	The disease-induced mortality rate of the infected humans	0.05	[26]
ϕ_1	The rate at which the exposed human population becomes infectious	0.2	Assumed
γ_1	The natural recovery rate of the human or host population	0.1428	[26]
β_1	The infectious rate of dengue virus from mosquitoes to susceptible humans	0.000024	Assumed
β_2	The infectious rate of dengue virus from infected human to vector population	0.000024	Assumed
θ_2	The rate at which the exposed vector population becomes infectious	0.2	Assumed
b	The average biting rate per vector per human	0.5, >1	[19], EE
τ	Delay measures	≥0	Assumed

$$\left.\frac{dI_2}{dt}\right|_{I_2=0} = \theta_2 E_2 - \mu_2 I_2 = \theta_2 E_2 \geq 0.$$

Since all the terms contributing to the rates of change are non-negative when the respective variable is zero, the positivity of the solutions is ensured for all $t \geq 0$, given non-negative initial conditions. □

Theorem 3.2. *Solutions of the system are all bounded in the feasible region* Ω.

Proof. Let the total populations $N_1(t)$ and $N_2(t)$ be as given in Equations (2.1) and (2.2), respectively. Summing the differential equations in each group give:

$$\frac{dN_1}{dt} = \frac{dS_1}{dt} + \frac{dE_1}{dt} + \frac{dI_1}{dt} + \frac{dR_1}{dt},$$
$$\frac{dN_2}{dt} = \frac{dS_2}{dt} + \frac{dE_2}{dt} + \frac{dI_2}{dt}.$$

Substituting the right-hand sides of these equations leads to:

$$\frac{dN_1}{dt} = \Lambda - b\beta_1 S_1 I_2 e^{-\delta\tau} - \mu_1 S_1 + \gamma_1 I_1 - (\mu_1 + \gamma_1 + \xi_1) I_1,$$
$$\frac{dN_2}{dt} = \eta - b\beta_2 S_2 I_1 - \mu_2 S_2 + \theta_2 E_2 - \mu_2 I_2.$$

Simplifying the terms yield:

$$\frac{dN_1}{dt} = \Lambda - \mu_1 N_1 - \xi_1 I_1,$$
$$\frac{dN_2}{dt} = \eta - \mu_2 N_2,$$

which are linear differential equations of the form:

$$\frac{dN}{dt} = \Lambda - \mu N,$$

where $\Lambda = \Lambda$ for N_1 and $\Lambda = \eta$ for N_2. The solution is:

$$N(t) = \frac{\Lambda}{\mu} + \left(N(0) - \frac{\Lambda}{\mu}\right) e^{-\mu t}.$$

Therefore, for $N_1(t)$ and $N_2(t)$, we respectively have:

$$N_1(t) = \frac{\Lambda}{\mu_1} + \left(N_1(0) - \frac{\Lambda}{\mu_1}\right) e^{-(\mu_1+\xi_1)t},$$
$$N_2(t) = \frac{\eta}{\mu_2} + \left(N_2(0) - \frac{\eta}{\mu_2}\right) e^{-\mu_2 t}.$$

As $t \to \infty$, the exponential terms $e^{-(\mu_1+\xi_1)t}$ and $e^{-\mu_2 t}$ approach to zero, hence:

$$N_1(t) \to \frac{\Lambda}{\mu_1}, \quad N_2(t) \to \frac{\eta}{\mu_2}.$$

Thus, the populations for both groups remain bounded:

$$N_1(t) \leq \frac{\Lambda}{\mu_1}, \quad N_2(t) \leq \frac{\eta}{\mu_2}.$$

Therefore, the total population for each group satisfies:

$$0 < N_1(t) \leq \frac{\Lambda}{\mu_1}, \quad 0 < N_2(t) \leq \frac{\eta}{\mu_2}.$$

This ensures that all solutions remain within the feasible region Ω:

$$\Omega = \left\{ (S_1, E_1, I_1, R_1, S_2, E_2, I_2) \in \mathbb{R}^7_+ \;\middle|\; 0 < N_1(t) \leq \frac{\Lambda}{\mu_1}, \quad 0 < N_2(t) \leq \frac{\eta}{\mu_2} \right\}.$$

Thus, the solutions for the system are bounded in the feasible region. □

3.1. **Model Equilibrium Points.** This section presents the system using two types of equilibrium points, denoted by ε_0 and ε_1, representing the disease-free and endemic states, respectively:

$$\varepsilon_0 = (S_1^0, E_1^0, I_1^0, R_1^0, S_2^0, E_2^0, I_2^0) = (\frac{\Lambda}{\mu_1}, 0, 0, 0, \frac{\eta}{\mu_2}, 0, 0),$$
$$\varepsilon_1 = (S_1^*, E_1^*, I_1^*, R_1^*, S_2^*, E_2^*, I_2^*),$$

where

$$S_1^* = \frac{\Lambda}{b\beta_1 I_2 e^{-\delta\tau} + \mu_1}, \quad E_1^* = \frac{b\beta_1 S_1 I_2 e^{-\delta\tau}}{\mu_1 + \phi_1}, \quad I_1^* = \frac{\phi_1 E_1}{\mu_1 + \gamma_1 + \xi_1}, \quad R_1^* = \frac{\gamma_1 I_1}{\mu_1},$$

$$S_2^* = \frac{\eta}{b\beta_2 I_1 + \mu_2}, \quad E_2^* = \frac{\beta_2 b I_1 S_2}{\theta_2 + \mu_2}, \quad I_2^* = \frac{\theta_2 E_2}{\mu_2}.$$

4. Fundamental Reproduction Number

The system's behavior is investigated using the fundamental reproduction number, denoted as R_0. This number represents the average number of new infections generated by a single infected individual in a fully susceptible population during the infectious period [9, 46]. This threshold value serves as a critical indicator to assess whether a disease will propagate or subside within a population. This can be determined using the next-generation matrix method. In this framework, the compartments representing the infected population are denoted as E_1, I_1, and I_2, while the non-infected population is represented by S_1, R_1, and S_2. The matrices G and H capture the infection generation rates and the transition rates between different stages, respectively. The next-generation matrix method [41] is applied to this system for analysis:

$$\frac{dx}{dt} = G(x, y) - H(x, y),$$

$$G = \begin{bmatrix} b\beta_1 S_1 I_2 e^{-\delta\tau} \\ 0 \\ \beta_2 b I_1 S_2 \\ 0 \end{bmatrix}, \quad H = \begin{bmatrix} (\phi_1 + \mu_1)E_1 \\ -\phi_1 E_1 + (\mu_1 + \gamma_1 + \xi_1)I_1 \\ (\theta_2 + \mu_2)E_2 \\ -\theta_2 E_2 + \mu_2 I_2 \end{bmatrix}.$$

Thus, at the disease-free equilibrium (DFE) points, both transmission matrices G and H are:

$$\bar{G} = \begin{bmatrix} 0 & 0 & 0 & b\beta_1 \frac{\Lambda}{\mu_1} e^{-\delta\tau} \\ 0 & 0 & 0 & 0 \\ 0 & b\frac{\eta}{\mu_2}\beta_2 & 0 & 0 \\ 0 & 0 & 0 & 0 \end{bmatrix}, \quad \bar{H} = \begin{bmatrix} \phi_1 + \mu_1 & 0 & 0 & 0 \\ -\phi_1 & \mu_1 + \gamma + \xi_1 & 0 & 0 \\ 0 & 0 & \theta_2 + \mu_2 & 0 \\ 0 & 0 & -\theta_2 & \mu_2 \end{bmatrix}.$$

Further calculations yield:

$$\bar{H}^{-1} = \begin{bmatrix} \frac{1}{\mu_1+\phi_1} & 0 & 0 & 0 \\ \frac{\theta_2\mu_2\phi_1 + \mu_2^2\phi_1}{\mu_2(\theta_2+\mu_2)(\mu_1+\phi_1)(\gamma+\mu_1+\xi_1)} & \frac{1}{\gamma+\mu_1+\xi_1} & 0 & 0 \\ 0 & 0 & \frac{1}{\theta_2+\mu_2} & 0 \\ 0 & 0 & \frac{\theta_2}{\mu_2(\theta_2+\mu_2)} & \frac{1}{\mu_2} \end{bmatrix},$$

$$\bar{G}\bar{H}^{-1} = \begin{bmatrix} 0 & 0 & \frac{b\beta_1\theta_2\Lambda e^{-\delta\tau}}{\mu_1\mu_2(\theta_2+\mu_2)} & \frac{b\beta_1\Lambda e^{-\delta\tau}}{\mu_1\mu_2} \\ 0 & 0 & 0 & 0 \\ \frac{b\beta_2\eta\left(\theta_2\mu_2\phi_1+\mu_2^2\phi_1\right)}{\mu_2^2(\theta_2+\mu_2)(\mu_1+\phi_1)(\gamma+\mu_1+\xi_1)} & \frac{b\beta_2\eta}{\mu_2(\gamma+\mu_1+\xi_1)} & 0 & 0 \\ 0 & 0 & 0 & 0 \end{bmatrix}.$$

Thus, the reproduction value corresponds to the largest spectral radius is

$$R_0 = \sqrt{\frac{b^2\beta_1\beta_2\eta\theta_2\Lambda\phi_1 e^{-\delta\tau}}{\mu_1\mu^2{}_2\left(\theta_2+\mu_2\right)\left(\mu_1+\phi_1\right)\left(\gamma+\mu_1+\xi_1\right)}}. \tag{4.1}$$

The spectral radius $\bar{G}\bar{H}^{-1}$ is assigned as the reproductive value and it is defined as R_0 in this model.

4.1. **Sensitivity Analysis of Parameters for Dengue Transmission.** Sensitivity analysis facilitates the identification of certain parameters that produce an impact on model outputs upon changes [38]. It enables the determination of critical parameters that substantially affect the results. By assessing the model's robustness, sensitivity analysis clarifies areas requiring more precise data or refined assumptions. Furthermore, it contributes to model validation, enhances the credibility of predictions, and supports informed decision-making by highlighting the most influential factors. Sensitivity analysis in epidemic models examines how modification in certain parameters affects the system's dynamics and results. By systematically adjusting these parametric values, researchers can assess how responsive the system's predictions are linked to each modification. This process helps pinpoint the parameters that most strongly influence the spread and management of the epidemic. The sensitivity analysis of the basic reproduction number R_0 with respect to each parameter is carried out. The partial derivatives of R_0 for all parameters are computed and analyzed on their effects using the following formula:

$$\text{Sensitivity index analysis} = \frac{\text{Parameter}}{R_0} \times \frac{\partial R_0}{\partial \text{Parameter}}, \tag{4.2}$$

The associated partial derivatives of R_0 are as follows:

$$\begin{aligned}
\frac{dR_0}{db} &= \frac{2b\beta_1\beta_2\eta\theta_2\Lambda\phi_1 e^{-\delta\tau}}{\mu_1\mu_2^2\left(\theta_2+\mu_2\right)\left(\mu_1+\phi_1\right)\left(\gamma+\mu_1+\xi_1\right)} > 0, \\
\frac{dR_0}{d\eta} &= \frac{b^2\beta_1\beta_2\theta_2\Lambda\phi_1 e^{-\delta\tau}}{\mu_1\mu_2^2\left(\theta_2+\mu_2\right)\left(\mu_1+\phi_1\right)\left(\gamma+\mu_1+\xi_1\right)} > 0, \\
\frac{dR_0}{d\Lambda} &= \frac{b^2\beta_1\beta_2\eta\theta_2\phi_1 e^{-\delta\tau}}{\mu_1\mu_2^2\left(\theta_2+\mu_2\right)\left(\mu_1+\phi_1\right)\left(\gamma+\mu_1+\xi_1\right)} > 0, \\
\frac{dR_0}{d\beta_1} &= \frac{b^2\beta_2\eta\theta_2\Lambda\phi_1 e^{-\delta\tau}}{\mu_1\mu_2^2\left(\theta_2+\mu_2\right)\left(\mu_1+\phi_1\right)\left(\gamma+\mu_1+\xi_1\right)} > 0, \\
\frac{dR_0}{d\beta_2} &= \frac{b^2\beta_1\eta\theta_2\Lambda\phi_1 e^{-\delta\tau}}{\mu_1\mu_2^2\left(\theta_2+\mu_2\right)\left(\mu_1+\phi_1\right)\left(\gamma+\mu_1+\xi_1\right)} > 0, \\
\frac{dR_0}{d\theta_2} &= \frac{b^2\beta_1\beta_2\eta\Lambda\phi_1 e^{-\delta\tau}}{\mu_1\mu_2\left(\theta_2+\mu_2\right)^2\left(\mu_1+\phi_1\right)\left(\gamma+\mu_1+\xi_1\right)} > 0, \\
\frac{dR_0}{d\phi_1} &= \frac{b^2\beta_1\beta_2\eta\theta_2\Lambda e^{-\delta\tau}}{\mu_2^2\left(\theta_2+\mu_2\right)\left(\mu_1+\phi_1\right)^2\left(\gamma+\mu_1+\xi_1\right)} > 0, \\
\frac{dR_0}{d\mu_1} &= -\frac{\left(\frac{1}{\gamma+\mu_1+\xi_1}+\frac{1}{\mu_1+\phi_1}+\frac{1}{\mu_1}\right)\left(b^2\beta_1\beta_2\eta\theta_2\Lambda\phi_1 e^{-\delta\tau}\right)}{\mu_1\mu_2^2\left(\theta_2+\mu_2\right)\left(\mu_1+\phi_1\right)\left(\gamma+\mu_1+\xi_1\right)} < 0, \\
\frac{dR_0}{d\mu_2} &= -\frac{b^2\beta_1\beta_2\eta\theta_2\Lambda\phi_1 e^{-\delta\tau}}{\mu_1\mu_2^2\left(\theta_2+\mu_2\right)^2\left(\mu_1+\phi_1\right)\left(\gamma+\mu_1+\xi_1\right)} < 0,
\end{aligned}$$

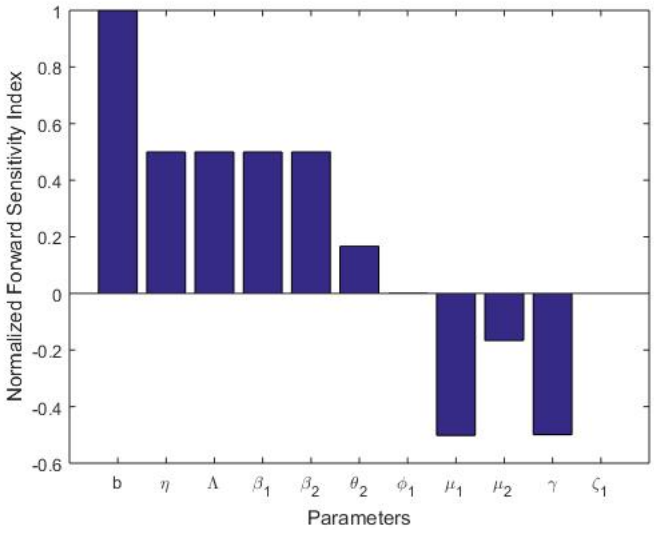

FIGURE 2. Sensitivity index.

$$\frac{dR_0}{d\gamma_1} = -\frac{b^2\beta_1\beta_2\eta\theta_2\Lambda\phi_1 e^{-\delta\tau}}{\mu_1\mu_2^2\left(\theta_2+\mu_2\right)\left(\mu_1+\phi_1\right)\left(\gamma+\mu_1+\xi_1\right)^2} < 0,$$

$$\frac{dR_0}{d\xi_1} = -\frac{b^2\beta_1\beta_2\eta\theta_2\Lambda\phi_1 e^{-\delta\tau}}{\mu_1\mu_2^2\left(\theta_2+\mu_2\right)\left(\mu_1+\phi_1\right)\left(\gamma+\mu_1+\xi_1\right)^2} < 0,$$

$$\frac{dR_0}{d\delta} < 0.$$

The R_0 value is influenced by the parameters involved in the model. The magnitude of each parameter's index determines whether R_0 will rise or fall in response to changes, as shown in Figure 2. A positive index indicates that an increase in the parameter will lead to an increase in the reproductive number, whereas a negative index suggests the opposite. Some parameters have positive sensitivity indices, indicating a direct relationship with R_0, while others have negative sensitivity indices, reflecting an inverse relationship. These results show that increasing parameters related to transmission, biting, and birth rates and decreasing parameters related to recovery, mortality, and transmission rates can have notable effects on the model's reproductive number. The sensitivity analysis of R_0 was performed to examine how different parameter pairs influence disease transmission. In Figure 3, the first case explores the relationship between the mosquito biting rate b and human recruitment rate Λ, where an increase in either parameter leads to a rise in R_0. This emphasizes the importance of reducing mosquito exposure and controlling human recruitment to minimize disease spread. The second case analyzes mosquito recruitment η and the infection transmission probability β_1, showing that increasing mosquito recruitment and an increased probability of infection significantly elevate R_0. This confirms the necessity of vector control measures such as larvicidal treatment and environmental sanitation. The third scenario examines the impact of the progression rate from exposed to infectious ϕ_1 and disease-induced mortality rate ξ_1, where a higher ϕ_1 increases R_0 due to a faster transition of individuals into the infectious state, whereas an increase in ξ_1 decreases R_0 by removing infected individuals from the population. This suggests that early medical interventions and improved healthcare access can alter the disease dynamics. Lastly, the fourth case investigates the effect of the incubation delay τ and the transition rate of exposed mosquitoes to the infectious stage θ_2, revealing that a longer incubation period τ reduces R_0, while an increase in θ_2 enhances transmission. These findings indicate that controlling environmental factors affecting mosquito development, such as temperature and humidity, could help mitigate disease transmission. Overall, the analysis underscores the significance of an integrated approach involving

vector control, public health interventions, and early treatment strategies to effectively reduce the spread of the disease. Furthermore, Figure 4 illustrates the impact of mosquito mortality μ_2 on the infected mosquito population I_2 over

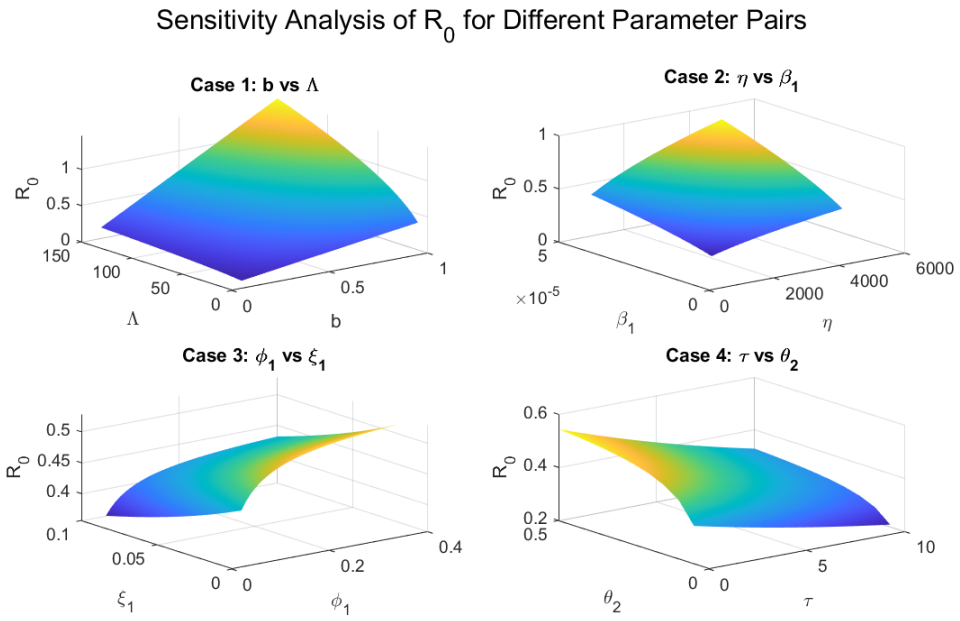

FIGURE 3. Sensitivity analysis of R_0 for selected pairs of parameters.

time. The results indicate that as the mosquito mortality rate increases, the number of infected mosquitoes decreases. This outcome aligns with the expected epidemiological behavior, where higher mosquito mortality reduces the vector population, ultimately limiting the transmission cycle. The decline in infection highlights the effectiveness of vector control strategies, such as insecticide-treated nets and environmental management, in reducing disease spread. Figure 5 presents the effect of human recruitment Λ on the infected human population I_1. As the recruitment rate increases, there is an initial rise in the number of infected individuals, suggesting that a higher influx of susceptible individuals into the population contributes to sustained transmission. However, depending on other epidemiological parameters such as recovery and control measures, the long-term infection dynamics may vary. This finding underscores the importance of considering population growth and human movement patterns when designing intervention strategies.

Figure 6(a) demonstrates the influence of two critical parameters, biting rate b and time delay τ, on the transmission dynamics of a vector-borne disease model. In the first figure, increasing the biting rate b from 0.1 to 0.7 significantly amplifies both populations of the infected human I_1 and mosquito I_2, leading to earlier and sharper infection peaks. This reflects the enhanced force of infection due to more frequent vector-host interactions as represented in the model equations. In contrast, Figure 6(b) explores the effect of introducing a time delay τ in the force of infection term $b\beta_1 S_1 I_2 e^{-\delta\tau}$. As τ increases, the infected human population experiences a substantial reduction in peak size and a delayed outbreak, indicating the dampening impact of delayed transmission on disease progression. Both parameters demonstrate the model's sensitivity to biological and behavioral mechanisms that govern the spread of infection. Thus, it is observed that parameters with a positive sensitivity index increase the disease transmission whereas the parameters with a negative sensitivity index decrease the transmission of the disease. In short, the numerical simulations have illustrated that variations in the biting rate and the incorporation of time delay significantly influence the infection dynamics. These results emphasize the sensitivity of the model to key transmission parameters and support the need for timely and targeted intervention strategies. Building upon these insights, the following section focuses on the analytical investigation of the model's local and global stability, providing a deeper understanding of the system's long-term behavior under various epidemiological conditions.

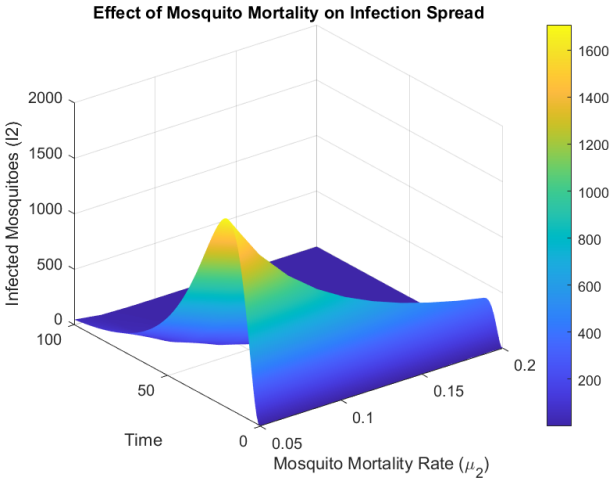

FIGURE 4. Effect of mosquito mortality μ_2 on infected mosquito population I_2.

FIGURE 5. Effect of human recruitment Λ on infected human population I_1.

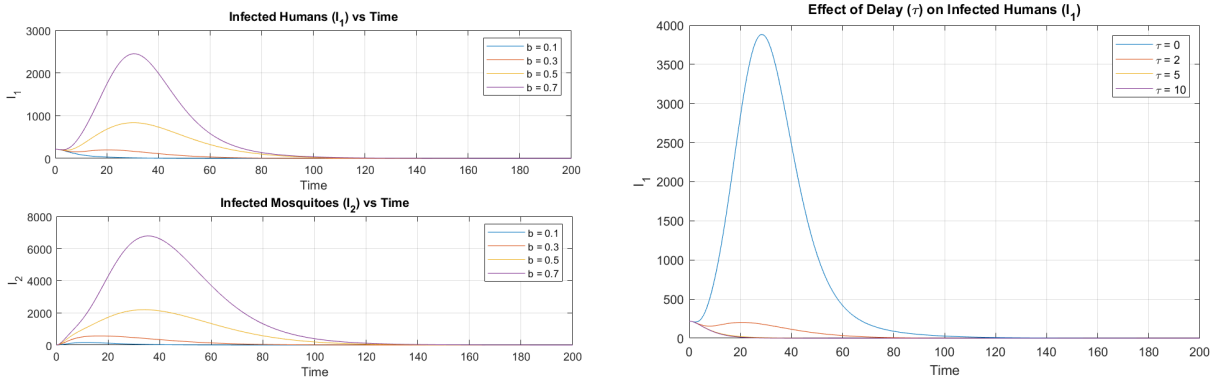

(a) (b)

FIGURE 6. Combined behavior of system with parametric values.

5. Stability Analysis

This section discusses the analysis of local and global stability at both DFE and endemic equilibrium (EE) points, employing the Routh-Hurwitz criterion and a Lyapunov function with certain properties.

5.1. **Local Stability.**

Theorem 5.1. *The system's DFE point, ε_0, is locally asymptotically stable when $R_0 < 1$.*

Proof. Linearizing the system with ε_0 leads to the Jacobian matrix approach:

$$J = \begin{bmatrix} -\mu_1 & 0 & 0 & 0 & 0 & 0 & -b\beta_1 e^{-\delta\tau}\frac{\Lambda}{\mu_1} \\ 0 & -\mu_1-\phi_1 & 0 & 0 & 0 & 0 & b\beta_1 e^{-\delta\tau}\frac{\Lambda}{\mu_1} \\ 0 & -\phi_1 & -\mu_1-\gamma_1-\xi_1 & 0 & 0 & 0 & 0 \\ 0 & 0 & \gamma_1 & -\mu_1 & 0 & 0 & 0 \\ 0 & 0 & -b\beta_2\frac{\eta}{\mu_2} & 0 & -\mu_2 & 0 & 0 \\ 0 & 0 & b\beta_2\frac{\eta}{\mu_2} & 0 & 0 & -\theta_2-\mu_2 & 0 \\ 0 & 0 & 0 & 0 & 0 & \theta_2 & -\mu_2 \end{bmatrix}.$$

Letting the characteristics equation $|J-\lambda I|=0$, we have:

$$\begin{vmatrix} -\mu_1-\lambda & 0 & 0 & 0 & 0 & 0 & -b\beta_1 e^{-\delta\tau}\frac{\Lambda}{\mu_1} \\ 0 & -\mu_1-\phi_1-\lambda & 0 & 0 & 0 & 0 & b\beta_1 e^{-\delta\tau}\frac{\Lambda}{\mu_1} \\ 0 & \phi_1 & -\mu_1-\gamma_1-\xi_1-\lambda & 0 & 0 & 0 & 0 \\ 0 & 0 & \gamma_1 & -\mu_1-\lambda & 0 & 0 & 0 \\ 0 & 0 & -b\beta_2\frac{\eta}{\mu_2} & 0 & -\mu_2-\lambda & 0 & 0 \\ 0 & 0 & b\beta_2\frac{\eta}{\mu_2} & 0 & 0 & -\theta_2-\mu_2-\lambda & 0 \\ 0 & 0 & 0 & 0 & 0 & \theta_2 & -\mu_2-\lambda \end{vmatrix} = 0.$$

From the matrix, some of the eigenvalues are directly determined as follows:

$$\lambda_1 = -\mu_1, \quad \lambda_2 = -\mu_1, \quad \lambda_3 = \mu_2.$$

We used Mathematica software and applied the Routh-Hurwitz criterion to verify that all values are negative. The remaining eigenvalues can be calculated from following the characteristics equation:

$$A_1\lambda^4 + A_2\lambda^3 + A_3\lambda^2 + A_4\lambda + A_5 = 0,$$

where

$$\begin{aligned}
A_1 &= 1, \\
A_2 &= \gamma_1+\theta_2+2\mu_1+2\mu_2+\xi_1+\phi_1, \\
A_3 &= \gamma_1\theta_2+\gamma_1\mu_1+2\gamma_1\mu_2+\gamma_1\phi_1+2\theta_2\mu_1+\theta_2\mu_2+\theta_2\xi_1+\theta_2\phi_1+{\mu_1}^2+4\mu_1\mu_2+\mu_1\xi_1+\mu_1\phi_1+{\mu_2}^2 \\
&\quad +2\mu_2\xi_1+2\mu_2\phi_1+\xi_1\varphi_1, \\
A_4 &= \gamma_1\theta_2\mu_1+\gamma_1\theta_2\mu_2+\gamma_1\theta_2\phi_1+2\gamma_1\mu_1\mu_2+\gamma_1{\mu_2}^2+2\gamma_1\mu_2\phi_1+\theta_2{\mu_1}^2+2\theta_2\mu_1\mu_2+\theta_2\mu_1\xi_1 \\
&\quad +\theta_2\mu_1\phi_1+\theta_2\mu_2\xi_1+\theta_2\mu_2\phi_1+\theta_2\xi_1\phi_1+2{\mu_1}^2\mu_2+2\mu_1{\mu_2}^2+2\mu_1\mu_2\xi_1+2\mu_1\mu_2\phi_1 \\
&\quad +{\mu_2}^2\xi_1+{\mu_2}^2\phi_1+2\mu_2\xi_1\phi_1, \\
A_5 &= \mu_2(\theta_2+\mu_2)(\mu_1+\phi_1)(\gamma_1+\mu_1+\xi_1)-\frac{b^2\beta_1\beta_2\eta\theta_2\Lambda\phi_1 e^{-\delta\tau}}{\mu_1\mu_2}.
\end{aligned}$$

A_5 can then be rewritten as:

$$\begin{aligned}
A_5 &= \mu_2(\theta_2+\mu_2)(\mu_1+\phi_1)(\gamma_1+\mu_1+\xi_1)\left(1-\frac{b^2\beta_1\beta_2\eta\theta_2\Lambda\phi_1 e^{-\delta\tau}}{\mu_1\mu_2^2(\theta_2+\mu_2)(\mu_1+\phi_1)(\gamma_1+\mu_1+\xi_1)}\right) \\
&= \mu_2(\theta_2+\mu_2)(\mu_1+\phi_1)(\gamma_1+\mu_1+\xi_1)\left(1-R_0^2\right).
\end{aligned}$$

Therefore,

$$A_5 > 0 \Leftrightarrow R_0 < 1.$$

Hence, by using the Routh-Hurwitz criterion, the DFE is ε_0 which proves the local asymptotic stability. □

Theorem 5.2. *If $R_0 > 1$, the system's endemic equilibrium point, ε_1, is locally asymptotically stable.*

Proof. Linearizing the system around ε_1 leads to the following Jacobian matrix:

$$J = \begin{bmatrix} -b\beta_1 I_2^* e^{-\delta\tau} - \mu_1 & 0 & 0 & 0 & 0 & 0 & -b\beta_1 S_1^* e^{-\delta\tau} \\ b\beta_1 I_2^* e^{-\delta\tau} & -\mu_1 - \phi_1 & 0 & 0 & 0 & 0 & b\beta_1 S_1^* e^{-\delta\tau} \\ 0 & \phi_1 & -\mu_1 - \gamma_1 - \xi_1 & 0 & 0 & 0 & 0 \\ 0 & 0 & \gamma_1 & -\mu_1 & 0 & 0 & 0 \\ 0 & 0 & -b\beta_2 S_2^* & 0 & -b\beta_2 I_1^* - \mu_2 & 0 & 0 \\ 0 & 0 & b\beta_2 S_2^* & 0 & b\beta_2 I_1^* & -\theta_2 - \mu_2 & 0 \\ 0 & 0 & 0 & 0 & 0 & -\theta_2 & -\mu_2 \end{bmatrix}.$$

Converting the matrix into lower triangular form:

$$J = \begin{bmatrix} -b\beta_1 I_2^* e^{-\delta\tau} - \mu_1 & 0 & 0 & 0 & 0 & 0 & 0 \\ b\beta_1 I_2^* e^{-\delta\tau} & -\mu_1 - \phi_1 & 0 & 0 & 0 & 0 & 0 \\ 0 & \phi_1 & -\mu_1 - \gamma_1 - \xi_1 & 0 & 0 & 0 & 0 \\ 0 & 0 & \gamma_1 & -\mu_1 & 0 & 0 & 0 \\ 0 & 0 & -b\beta_2 S_2^* & 0 & -b\beta_2 I_1^* - \mu_2 & 0 & 0 \\ 0 & 0 & b\beta_2 S_2^* & 0 & b\beta_2 I_1^* & -\theta_2 - \mu_2 & 0 \\ 0 & 0 & 0 & 0 & 0 & -\theta_2 & -\mu_2 \end{bmatrix},$$

the eigenvalues of a lower triangular matrix are the entries along the main diagonal. Thus, the eigenvalues of J are:

$$\lambda_1 = -b\beta_1 I_2^* e^{-\delta\tau} - \mu_1, \quad \lambda_2 = -\mu_1 - \phi_1, \quad \lambda_3 = -\mu_1 - \gamma_1 - \xi_1, \quad \lambda_4 = -\mu_1,$$
$$\lambda_5 = -b\beta_2 I_1^* - \mu_2, \quad \lambda_6 = -\theta_2 - \mu_2, \quad \lambda_7 = -\mu_2$$

Since all diagonal values are negative, the endemic points are asymptotically stable. □

5.2. **Global Stability.**

Theorem 5.3. *The DFE point $\varepsilon_0 = \left(\frac{\Lambda}{\mu_1}, 0, 0, 0, \frac{\eta}{\mu_2}, 0, 0\right)$ of the given system is globally asymptotically stable (GAS) when $R_0 < 1$ and unstable when $R_0 > 1$.*

Proof. Consider a Volterra-type Lyapunov function [32, 33, 37] $U : \Omega \to \mathbb{R}$:

$$U = S_1 - S_1^0 \ln S_1 + E_1 + I_1 + R_1 + S_2 - S_2^0 \ln S_2 + E_2 + I_2.$$

Computing the time derivative of U:

$$\dot{U} = \left(1 - \frac{S_1^0}{S_1}\right)\dot{S}_1 + \dot{E}_1 + \dot{I}_1 + \dot{R}_1 + \left(1 - \frac{S_2^0}{S_2}\right)\dot{S}_2 + \dot{E}_2 + \dot{I}_2,$$

and substituting the model equations for the given system yield:

$$\begin{aligned}
\dot{S}_1 &= \Lambda - b\beta_1 S_1 I_2 e^{-\delta\tau} - \mu_1 S_1,\\
\dot{E}_1 &= b\beta_1 S_1 I_2 e^{-\delta\tau} - (\mu_1+\phi_1)E_1,\\
\dot{I}_1 &= \phi_1 E_1 - (\mu_1+\gamma_1+\xi_1)I_1,\\
\dot{R}_1 &= \gamma_1 I_1 - \mu_1 R_1,\\
\dot{S}_2 &= \eta - b\beta_2 S_2 I_1 - \mu_2 S_2,\\
\dot{E}_2 &= b\beta_2 S_2 I_1 - (\theta_2+\mu_2)E_2,\\
\dot{I}_2 &= \theta_2 E_2 - \mu_2 I_2.
\end{aligned}$$

Substituting the latter equations into $\dot{U}$, we obtain:

$$\begin{aligned}
\dot{U} = &\left(1-\frac{S_1^0}{S_1}\right)\left[\Lambda - b\beta_1 S_1 I_2 e^{-\delta\tau} - \mu_1 S_1\right] + \left[b\beta_1 S_1 I_2 e^{-\delta\tau} - (\mu_1+\phi_1)E_1\right]\\
&+ \left[\phi_1 E_1 - (\mu_1+\gamma_1+\xi_1)I_1\right] + \left[\gamma_1 I_1 - \mu_1 R_1\right] + \left(1-\frac{S_2^0}{S_2}\right)\left[\eta - b\beta_2 S_2 I_1 - \mu_2 S_2\right]\\
&+ \left[b\beta_2 S_2 I_1 - (\theta_2+\mu_2)E_2\right] + \left[\theta_2 E_2 - \mu_2 I_2\right].
\end{aligned}$$

Let$S_1^0 = \frac{\Lambda}{\mu_1}$ and $S_2^0 = \frac{\eta}{\mu_2}$. Then, $\dot{U}$ is simplified into:

$$\begin{aligned}
\dot{U} = &-\frac{\mu_1}{S_1}\left(S_1 - S_1^0\right)^2 - (\mu_1+\phi_1)E_1 - (\mu_1+\gamma_1+\xi_1)I_1 - \mu_1 R_1 - \frac{\mu_2}{S_2}\left(S_2 - S_2^0\right)^2\\
&- (\mu_2+\theta_2)E_2 - \mu_2 I_2 + \frac{S_1^0}{S_1} b\beta_1 S_1 I_2 e^{-\delta\tau} + \frac{S_2^0}{S_2} b\beta_2 S_2 I_1.
\end{aligned}$$

We now analyze $\dot{U}$. For $R_0 < 1$, we have:

$$b\beta_1 e^{-\delta\tau} < \mu_1, \quad \text{and} \quad b\beta_2 < \mu_2.$$

Thus:

$$\dot{U} \leq 0.$$

Equality holds ($\dot{U} = 0$) if and only if:

$$S_1 = S_1^0, \quad S_2 = S_2^0, \quad E_1 = 0, \quad I_1 = 0, \quad R_1 = 0, \quad E_2 = 0, \quad I_2 = 0.$$

Hence, the DFE ε_0 is GAS when $R_0 < 1$. □

Theorem 5.4. *For $R_0 > 1$, the system is GAS at the indicated point ε_1.*

Proof. Suppose $\mathcal{R}_0 > 1$. The Lyapunov function $\mathcal{L} : \mathbf{R}_+^7 \to \mathbf{R}_+$ is constructed by the following formula:

$$\mathcal{L} = \frac{1}{2}\left[(S_1 - S_1^*) + (E_1 - E_1^*) + (I_1 - I_1^*) + (R_1 - R_1^*)\right]^2 + \frac{1}{2}\left[(S_2 - S_2^*) + (E_2 - E_2^*) + (I_2 - I_2^*)\right]^2.$$

Differentiating $\mathcal{L}$ with respect to t,

$$\begin{aligned}
\dot{\mathcal{L}} = &\left[(S_1 - S_1^*) + (E_1 - E_1^*) + (I_1 - I_1^*) + (R_1 - R_1^*)\right] \cdot \frac{d}{dt}(S_1 + E_1 + I_1 + R_1)\\
&+ \left[(S_2 - S_2^*) + (E_2 - E_2^*) + (I_2 - I_2^*)\right] \cdot \frac{d}{dt}(S_2 + E_2 + I_2),
\end{aligned}$$

and substituting the system's dynamics yield:

$$\begin{aligned}
\dot{\mathcal{L}} = &\left[(S_1 - S_1^*) + (E_1 - E_1^*) + (I_1 - I_1^*) + (R_1 - R_1^*)\right] \cdot \left[\Lambda - \mu_1(S_1 + E_1 + I_1 + R_1) - \xi_1 I_1\right]\\
&+ \left[(S_2 - S_2^*) + (E_2 - E_2^*) + (I_2 - I_2^*)\right] \cdot \left[\eta - \mu_2(S_2 + E_2 + I_2)\right].
\end{aligned}$$

Using the limiting relations $N_1 \leq \frac{\Lambda}{\mu_1}$ and $N_2 \leq \frac{\eta}{\mu_2}$, we have:

$$\begin{aligned}\dot{\mathcal{L}} \leq & -\mu_1 \left[(S_1 - S_1^*) + (E_1 - E_1^*) + (I_1 - I_1^*) + (R_1 - R_1^*)\right] \cdot \left[(S_1 + E_1 + I_1 + R_1) - (S_1^* + E_1^* + I_1^* + R_1^*)\right] \\ & - \mu_2 \left[(S_2 - S_2^*) + (E_2 - E_2^*) + (I_2 - I_2^*)\right] \cdot \left[(S_2 + E_2 + I_2) - (S_2^* + E_2^* + I_2^*)\right].\end{aligned}$$

Thus,

$$\dot{\mathcal{L}} \leq -\mu_1 \left[(S_1 - S_1^*) + (E_1 - E_1^*) + (I_1 - I_1^*) + (R_1 - R_1^*)\right]^2 - \mu_2 \left[(S_2 - S_2^*) + (E_2 - E_2^*) + (I_2 - I_2^*)\right]^2.$$

Therefore, $\dot{\mathcal{L}} \leq 0$ and $\dot{\mathcal{L}} = 0$ if and only if:

$$S_1 = S_1^*, \quad E_1 = E_1^*, \quad I_1 = I_1^*, \quad R_1 = R_1^*, \quad S_2 = S_2^*, \quad E_2 = E_2^*, \quad I_2 = I_2^*.$$

Therefore, the largest invariant set in $\left\{(S_1, E_1, I_1, R_1, S_2, E_2, I_2) \in \Omega : \frac{d\mathcal{L}}{dt} = 0\right\}$ is the equilibrium point. By LaSalle's Invariance Principle, the system is GAS in Ω. □

Now, we present the numerical analysis of the proposed model to validate the theoretical findings and illustrate the dynamic behavior of the system.

6. Numerical Analysis

Numerical methods play a crucial role in solving differential equations, with each technique offering distinct advantages depending on the problem's nature. The Runge-Kutta fourth-order (RK4) method is a widely used explicit scheme known for its high accuracy and stability in handling smooth, continuous systems. In contrast, the Non-standard Finite Difference (NSFD) method incorporates innovative discretization rules that often preserve the key physical properties, such as positivity and conservation laws, making it particularly effective for problems where traditional methods fail. In this study, we applied the RK4 and NSFD methods to solve an epidemiological model. While RK4 offers highly accurate results, they can diverge at certain points, limiting its reliability for complex systems. In contrast, the NSFD method remains stable and convergent, ensuring more accurate and biologically realistic results. This makes NSFD a more reliable choice for simulating disease dynamics and evaluating control strategies. Here, we investigate two finite difference schemes to analyze the dynamical behavior of the system, specifically employing the NSFD method to effectively handle its complexities. Furthermore, we will look at the stability of the NSFD method at the DFE point of the SEIR-SI model.

6.1. Runge-Kutta Rourth-Order Method.

The explicit RK4 scheme is applied on the SEIR-SEI system as follows:

$$\begin{aligned}k_1 &= h\left[\Lambda - b\beta_1 S_1^n I_2^n e^{-\delta\tau} - \mu_1 S_1^n\right], \\ l_1 &= h\left[b\beta_1 S_1^n I_2^n e^{-\delta\tau} - (\mu_1 + \phi_1) E_1^n\right], \\ m_1 &= h\left[E_1^n \phi_1 - (\mu_1 + \gamma_1 + \xi_1) I_1^n\right], \\ n_1 &= h\left[\gamma_1 I_1^n - \mu_1 R_1^n\right], \\ o_1 &= h\left[\eta - b\beta_2 S_2^n I_1^n - \mu_2 S_2^n\right], \\ p_1 &= h\left[b\beta_2 I_1^n S_2^n - (\theta_2 + \mu_2) E_2^n\right], \\ q_1 &= h\left[\theta_2 E_2^n - \mu_2 I_2^n\right],\end{aligned}$$

$$\begin{aligned}k_2 &= h\left[\Lambda - b\beta_1 \left(S_1^n + \frac{k_1}{2}\right)\left(I_2^n + \frac{q_1}{2}\right) e^{-\delta\tau} - \mu_1 \left(S_1^n + \frac{k_1}{2}\right)\right], \\ l_2 &= h\left[b\beta_1 \left(S_1^n + \frac{k_1}{2}\right)\left(I_2^n + \frac{q_1}{2}\right) e^{-\delta\tau} - (\mu_1 + \phi_1)\left(E_1^n + \frac{l_1}{2}\right)\right], \\ m_2 &= h\left[\phi_1 \left(E_1^n + \frac{l_1}{2}\right) - (\mu_1 + \gamma_1 + \xi_1)\left(I_1^n + \frac{m_1}{2}\right)\right], \\ n_2 &= h\left[\gamma_1 \left(I_1^n + \frac{m_1}{2}\right) - \mu_1 \left(R_1^n + \frac{n_1}{2}\right)\right], \\ o_2 &= h\left[\eta - b\beta_2 \left(S_2^n + \frac{o_1}{2}\right)\left(I_1^n + \frac{m_1}{2}\right) - \mu_2 \left(S_2^n + \frac{o_1}{2}\right)\right],\end{aligned}$$

$$
\begin{aligned}
p_2 &= h\left[b\beta_2\left(S_2^n+\frac{o_1}{2}\right)\left(I_1^n+\frac{m_1}{2}\right)-(\theta_2+\mu_2)\left(E_2^n+\frac{p_1}{2}\right)\right],\\
q_2 &= h\left[\theta_2\left(E_2^n+\frac{p_1}{2}\right)-\mu_2\left(I_2^n+\frac{q_1}{2}\right)\right],\\
k_3 &= h\left[\Lambda-b\beta_1\left(S_1^n+\frac{k_2}{2}\right)\left(I_2^n+\frac{q_2}{2}\right)e^{-\delta\tau}-\mu_1\left(S_1^n+\frac{k_2}{2}\right)\right],\\
l_3 &= h\left[b\beta_1\left(S_1^n+\frac{k_2}{2}\right)\left(I_2^n+\frac{q_2}{2}\right)e^{-\delta\tau}-(\mu_1+\phi_1)\left(E_1^n+\frac{l_2}{2}\right)\right],\\
m_3 &= h\left[\phi_1\left(E_1^n+\frac{l_2}{2}\right)-(\mu_1+\gamma_1+\xi_1)\left(I_1^n+\frac{m_2}{2}\right)\right],\\
n_3 &= h\left[\gamma_1\left(I_1^n+\frac{m_2}{2}\right)-\mu_1\left(R_1^n+\frac{n_2}{2}\right)\right],\\
o_3 &= h\left[\eta-b\beta_2\left(S_2^n+\frac{o_2}{2}\right)\left(I_1^n+\frac{m_2}{2}\right)-\mu_2\left(S_2^n+\frac{o_2}{2}\right)\right],\\
p_3 &= h\left[b\beta_2\left(I_1^n+\frac{m_2}{2}\right)\left(S_2^n+\frac{o_2}{2}\right)-(\theta_2+\mu_2)\left(E_2^n+\frac{p_2}{2}\right)\right],\\
q_3 &= h\left[\theta_2\left(E_2^n+\frac{p_2}{2}\right)-\mu_2\left(I_2^n+\frac{q_2}{2}\right)\right],\\
k_4 &= h\left[\Lambda-b\beta_1\left(S_1^n+k_3\right)\left(I_2^n+q_3\right)e^{-\delta\tau}-\mu_1\left(S_1^n+k_3\right)\right],\\
l_4 &= h\left[b\beta_1\left(S_1^n+k_3\right)\left(I_2^n+q_3\right)e^{-\delta\tau}-(\mu_1+\phi_1)\left(E_1^n+l_3\right)\right],\\
m_4 &= h\left[\phi_1\left(E_1^n+l_3\right)-(\mu_1+\gamma_1+\xi_1)\left(I_1^n+m_3\right)\right],\\
n_4 &= h\left[\gamma_1\left(I_1^n+m_3\right)-\mu_1\left(R_1^n+n_3\right)\right],\\
o_4 &= h\left[\eta-b\beta_2\left(S_2^n+o_3\right)+\left(I_1^n+m_3\right)-\mu_2\left(S_2^n+o_3\right)\right],\\
p_4 &= h\left[b\beta_2\left(S_2^n+o_3\right)\left(I_1^n+m_3\right)-(\theta_2+\mu_2)\left(E_2^n+p_3\right)\right],\\
q_4 &= h\left[\theta_2\left(E_2^n+p_3\right)-\mu_2\left(I_2^n+q_3\right)\right].
\end{aligned}
$$

Therefore, the recursive formulas for the numerical solutions are:

$$S_1^{n+1} = S_1^n + \frac{1}{6}[k_1+2k_2+2k_3+k_4], \tag{6.1a}$$

$$E_1^{n+1} = E_1^n + \frac{1}{6}[l_1+2l_2+2l_3+l_4], \tag{6.1b}$$

$$I_1^{n+1} = I_1^n + \frac{1}{6}[m_1+2m_2+2m_3+m_4], \tag{6.1c}$$

$$R_1^{n+1} = R_1^n + \frac{1}{6}[n_1+2n_2+2n_3+n_4], \tag{6.1d}$$

$$S_2^{n+1} = S_2^n + \frac{1}{6}[o_1+2o_2+2o_3+o_4], \tag{6.1e}$$

$$E_2^{n+1} = I_2^n + \frac{1}{6}[p_1+2p_2+2p_3+p_4], \tag{6.1f}$$

$$I_2^{n+1} = I_2^n + \frac{1}{6}[q_1+2q_2+2q_3+q_4], \tag{6.1g}$$

where h is the step size and $n = 0, 1, \ldots$.

6.2. **Non-Standard Finite Difference Method.** This section covers the formulation of the NSFD method along with its convergence and consistency analyses. These analyses are crucial for ensuring the reliability and accuracy of the method in solving epidemiological models. Convergence refers to the ability of the numerical solution to approach the exact solution as the step size tends to zero, while consistency ensures that the method approximates the differential equation correctly at each step. Through rigorous convergence and consistency analysess, we can confirm that the

NSFD method provides accurate and stable solutions even for complex, nonlinear systems, thus ensuring its robustness in modeling disease dynamics. Discretizing Equation (2.3a) using the NSFD scheme yield:

$$\frac{S_1^{n+1}-S_1^n}{h} = \Lambda - b\beta_1 S_1^{n+1} I_2^n e^{-\delta\tau} - \mu_1 S_1^{n+1},$$

where h is the step size and n is the number of iterations as $n = 0, 1, 2, 3, 4.....$ Rearranging the equation, we obtain Equation (6.2a). Similarly, Equations (2.3b) to (2.3g) are discretized resulting in Equations (6.2b) to (6.2g), respectively.

$$S_1^{n+1} = \frac{S_1^n + h\Lambda}{1 + hb\beta_1 I_2^n e^{-\delta\tau} + h\mu_1}, \tag{6.2a}$$

$$E_1^{n+1} = \frac{E_1^n + hb\beta_1 S_1^n I_2^n e^{-\delta\tau}}{1 + h(\mu_1 + \phi_1)}, \tag{6.2b}$$

$$I_1^{n+1} = \frac{I_1^n + h\phi_1 E_1^n}{1 + h(\mu_1 + \gamma_1 + \xi_1)}, \tag{6.2c}$$

$$R_1^{n+1} = \frac{R_1^n + h\gamma_1 I_1^n}{1 + h\mu_1}, \tag{6.2d}$$

$$S_2^{n+1} = \frac{S_2^n + h\eta}{1 + hb\beta_2 I_1^n + h\mu_2}, \tag{6.2e}$$

$$E_2^{n+1} = \frac{E_2^n + hb\beta_2 S_2^n I_1^n}{1 + h(\theta_2 + \mu_2)}, \tag{6.2f}$$

$$I_2^{n+1} = \frac{I_2^n + h\theta_2 E_2^n}{1 + h\mu_2}. \tag{6.2g}$$

6.2.1. *Convergence Analysis.*

Theorem 6.1 (Positivity)**.** *There is only one positive solution,* $(S_1, E_1, I_1, R_1, S_2, E_2, I_2) \in \mathbb{R}_7^+$*, for all* $n \geq 0$ *for any initial value* $(S_1(0), E_1(0), I_1(0), R_1(0), S_2(0), E_2(0), I_2(0)) \in \mathbb{R}_7^+$*.*

Proof. The conclusion holds for $n = 0$ based on the given hypotheses. Assuming that the conclusion is valid for some $n \geq 1$, it can be observed that the right-hand side of each NSFD equation remains positive when all of the parameters are positive. It follows that all the entries of S_1^{n+1}, E_1^{n+1}, I_1^{n+1}, R_1^{n+1}, S_2^{n+1}, E_2^{n+1}, and I_2^{n+1} are positive numbers. By mathematical induction, the positivity is proven. □

In this segment, convergence analysis of NSFD will be done at the DFE points $\varepsilon_0 = \left(\frac{\Lambda}{\mu_1}, 0, 0, 0, \frac{\eta}{\mu_2}, 0, 0\right)$. Suppose we have the following:

$$C = S_1^{n+1} = \frac{S_1^n + h\Lambda}{1 + hb\beta_1 I_2^n e^{-\delta\tau} + h\mu_1}, \quad D = E_1^{n+1} = \frac{E_1^n + hb\beta_1 S_1^n I_2^n e^{-\delta\tau}}{1 + h(\mu_1 + \phi_1)},$$

$$F = I_1^{n+1} = \frac{I_1^n + h\phi_1 E_1^n}{1 + h(\mu_1 + \gamma_1 + \xi_1)}, \quad G = R_1^{n+1} = \frac{R_1^n + h\gamma_1 I_1^n}{1 + h\mu_1},$$

$$H = S_2^{n+1} = \frac{S_2^n + h\eta}{1 + hb\beta_2 I_1^n + h\mu_2}, \quad J = E_2^{n+1} = \frac{E_2^n + hb\beta_2 I_1^n S_2^n}{1 + h(\theta_2 + \mu_2)},$$

$$K = I_2^{n+1} = \frac{I_2^n + h\theta_2 E_2^n}{1 + h\mu_2}.$$

Differentiating C, D, F, G, H, and J with respect to S_1, E_1, I_1, R_1, S_2, E_2, and I_2, we obtain the following Jacobian matrix of the equations:

$$J = \begin{bmatrix} C_{S_1} & C_{E_1} & C_{I_1} & C_{R_1} & C_{S_2} & C_{E_2} & C_{I_2} \\ D_{S_1} & D_{E_1} & D_{I_1} & D_{R_1} & D_{S_2} & D_{E_2} & D_{I_2} \\ F_{S_1} & F_{E_1} & F_{I_1} & F_{R_1} & F_{S_2} & F_{E_2} & F_{I_2} \\ G_{S_1} & G_{E_1} & G_{I_1} & G_{R_1} & G_{S_2} & G_{E_2} & G_{I_2} \\ H_{S_1} & H_{E_1} & H_{I_1} & H_{R_1} & H_{S_2} & H_{E_2} & H_{I_2} \\ J_{S_1} & J_{E_1} & J_{I_1} & J_{R_1} & J_{S_2} & J_{E_2} & J_{I_2} \\ K_{S_1} & K_{E_1} & J_{I_1} & K_{R_1} & K_{S_2} & K_{E_2} & K_{I_2} \end{bmatrix},$$

Substituting the values into J yield:

$$J = \begin{bmatrix} \frac{1}{1+h\mu_1} & 0 & 0 & 0 & 0 & 0 & \frac{\frac{\Lambda}{\mu_1}(-hb\beta_1 e^{-\delta\tau})}{1+h\mu_1} \\ 0 & \frac{1}{1+h(\mu_1+\phi_1)} & 0 & 0 & 0 & 0 & \frac{\frac{\Lambda}{\mu_1}(hb\beta_1 e^{-\delta\tau})}{1+h(\mu_1+\phi_1)} \\ 0 & \frac{h\phi_1}{1+h(\mu_1+\gamma_1+\xi_1)} & \frac{1}{1+h(\mu_1+\gamma_1+\xi_1)} & 0 & 0 & 0 & 0 \\ 0 & 0 & \frac{h\gamma_1}{1+h\mu_1} & \frac{1}{1+h\mu_1} & 0 & 0 & 0 \\ 0 & 0 & \frac{\frac{\eta}{\mu_2}-hb\beta_2}{1+h\mu_2} & 0 & \frac{1}{1+h\mu_2} & 0 & 0 \\ 0 & 0 & \frac{\frac{\eta}{\mu_2}(hb\beta_2)}{1+h(\theta_2+\mu_2)} & 0 & 0 & \frac{1}{1+h(\theta_2+\mu_2)} & 0 \\ 0 & 0 & 0 & 0 & 0 & \frac{h\theta_2}{1+h\mu_2} & \frac{1}{1+h\mu_2} \end{bmatrix}.$$

Taking $det(J - \lambda I) = 0$,

$$\begin{vmatrix} \frac{1}{1+h\mu_1}-\lambda & 0 & 0 & 0 & 0 & 0 & \frac{\frac{\Lambda}{\mu_1}(-hb\beta_1 e^{-\delta\tau})}{1+h\mu_1} \\ 0 & \frac{1}{1+h(\mu_1+\phi_1)}-\lambda & 0 & 0 & 0 & 0 & \frac{\frac{\Lambda}{\mu_1}(hb\beta_1 e^{-\delta\tau})}{1+h(\mu_1+\phi_1)} \\ 0 & \frac{h\phi_1}{1+h(\mu_1+\gamma_1+\xi_1)} & \frac{1}{1+h(\mu_1+\gamma_1+\xi_1)}-\lambda & 0 & 0 & 0 & 0 \\ 0 & 0 & \frac{h\gamma_1}{1+h\mu_1} & \frac{1}{1+h\mu_1}-\lambda & 0 & 0 & 0 \\ 0 & 0 & \frac{\frac{\eta}{\mu_2}-hb\beta_2}{1+h\mu_2} & 0 & \frac{1}{1+h\mu_2}-\lambda & 0 & 0 \\ 0 & 0 & \frac{\frac{\eta}{\mu_2}(hb\beta_2)}{1+h(\theta_2+\mu_2)} & 0 & 0 & \frac{1}{1+h(\theta_2+\mu_2)}-\lambda & 0 \\ 0 & 0 & 0 & 0 & 0 & \frac{h\theta_2}{1+h\mu_2} & \frac{1}{1+h\mu_2}-\lambda \end{vmatrix},$$

after putting it equal to zero and taking determinant three of its eigenvalues are $\frac{1}{h+\mu_1}$, $\frac{1}{h+\mu_1}$, and $\frac{1}{h+\mu_2}$. Using Mathematica, the remaining matrix are obtained as follows:

$$\begin{vmatrix} \frac{1}{1+h(\mu_1+\phi_1)}-\lambda & 0 & 0 & \frac{\frac{\Lambda}{\mu_1}(-hb\beta_1 e^{-\delta\tau})}{1+h\mu_1} \\ \frac{h\phi_1}{1+h(\mu_1+\gamma_1+\xi_1)} & \frac{1}{1+h(\mu_1+\gamma_1+\xi_1)}-\lambda & 0 & 0 \\ 0 & \frac{\frac{\eta}{\mu_2}(hb\beta_2)}{1+h(\theta_2+\mu_2)} & \frac{1}{1+h(\theta_2+\mu_2)}-\lambda & 0 \\ 0 & 0 & \frac{h\theta_2}{1+h\mu_2} & \frac{1}{1+h\mu_2}-\lambda \end{vmatrix} = 0.$$

The rest of the values were analyzed by Mathematica and they satisfied the condition. Therefore, our scheme is convergent.

6.2.2. *Consistency Analysis.* In this section, consistency of the numerical method is examined by employing the expansion of a Taylor series. We begin by selecting the first equation from the numerical integration model and expanding it using Taylor's series for S^{n+1}.

$$S_1^{n+1} = S_1^n + h\frac{dS_1}{dt} + \frac{h^2}{2!}\frac{d^2S_1}{dt^2} + \frac{h^3}{3!}\frac{d^3S_1}{dt^3} + \cdots . \tag{6.3}$$

Then,

$$\begin{aligned}
&S_1^{n+1}(1+hb\beta_1 I_2^n e^{-\delta\tau}+h\mu_1) = S_1^n + h\Lambda,\\
&\left(S_1^n + h\frac{dS_1}{dt} + \frac{h^2}{2!}\frac{d^2S_1}{dt^2} + \frac{h^3}{3!}\frac{d^3S_1}{dt^3} + \cdots\right)(1+hb\beta_1 I_2^n e^{-\delta\tau}+h\mu_1) = S_1^n + h\Lambda,\\
&S_1^n + hS_1^n b\beta_1 I_2^n e^{-\delta\tau} + S_1^n h\mu_1 + h\frac{dS_1}{dt} + h^2\frac{dS_1}{dt}b\beta_1 I_1^n e^{-\delta\tau} + h^2\mu_1\frac{dS_1}{dt}\\
&\quad + \left(\frac{h^2}{2!}\frac{d^2S_1}{dt^2} + \frac{h^3}{3!}\frac{d^3S_1}{dt^3} + \cdots\right)(1+hb\beta_1 I_2^n e^{-\delta\tau}+h\mu_1) = S_1^n + h\Lambda,\\
&h\left(S_1^n b\beta_1 I_2^n e^{-\delta\tau} + S_1^n\mu_1 + \frac{dS_1}{dt} + h\frac{dS_1}{dt}b\beta_1 I_2^n e^{-\delta\tau} + h\mu_1\frac{dS_1}{dt}\right)\\
&\quad + \left(\frac{h}{2!}\frac{d^2S_1}{dt^2} + \frac{h^2}{3!}\frac{d^3S_1}{dt^3} + \cdots\right)(1+hb\beta_1 I_2^n e^{-\delta\tau}+h\mu_1) = h\Lambda.
\end{aligned}$$

We obtain as follows:

$$\begin{aligned}
&S_1^n b\beta_1 I_2^n e^{-\delta\tau} + S_1^n\mu_1 + \frac{dS_1}{dt} + h\frac{dS_1}{dt}b\beta_1 I_1^n e^{-\delta\tau} + h\mu_1\frac{dS_1}{dt}\\
&\quad + \left(\frac{h}{2!}\frac{d^2S_1}{dt^2} + \frac{h^2}{3!}\frac{d^3S_1}{dt^3} + \cdots\right)(1+hb\beta_1 I_2^n e^{-\delta\tau}+h\mu_1) = \Lambda.
\end{aligned} \tag{6.4}$$

Taking $h \to 0$ yield

$$\begin{aligned}
&S_1^n b\beta_1 I_2^n e^{-\delta\tau} + S_1^n\mu_1 + \frac{dS_1}{dt} = \Lambda,\\
\Longrightarrow\ &\frac{dS_1}{dt} = \Lambda - S_1^n b\beta_1 I_2^n e^{-\delta\tau} - S_1^n\mu_1.
\end{aligned} \tag{6.5}$$

This outcome suggests that the discretized equation aligns with Equation (2.3a) from the model.

Similarly, Taylor expansion is applied on E_1^{n+1}, from Equation (2.3b),

$$E_1^{n+1} = E_1^n + h\frac{dE_1}{dt} + \frac{h^2}{2!}\frac{d^2E_1}{dt^2} + \frac{h^3}{3!}\frac{d^3E_1}{dt^3} + \cdots . \tag{6.6}$$

From the following expression,

$$E_1^{n+1}(1+h(\mu_1+\phi_1)) = E_1^n + hb\beta_1 S_1^n I_2^n e^{-\delta\tau}, \tag{6.7}$$

we obtain

$$\begin{aligned} &E_1^n + E_1^n h(\mu_1+\phi_1) + h\frac{dE_1}{dt} + h^2(\mu_1+\phi_1)\frac{dE_1}{dt} + \left(\frac{h^2}{2!}\frac{d^2E_1}{dt^2} + \frac{h^3}{3!}\frac{d^3E}{dt^3} + \cdots\right) \\ &\quad \times (1+h(\mu_1+\phi_1)) = E_1^n + hb\beta_1 S_1^n I_2^n e^{-\delta\tau}. \end{aligned} \tag{6.8}$$

Then, as $h \to 0$, we have

$$\frac{dE_1}{dt} = b\beta_1 S_1^n I_2^n e^{-\delta\tau} - (\mu_1+\phi_1)E_1^n. \tag{6.9}$$

Analogous to the calculations for S_1^{n+1} and E_1^{n+1}, applying Taylor's series expansion on I_1^{n+1}, R^{n+1}, I_1^{n+1}, E_2^{n+1}, and I_S^{n+1} respectively from equations (2.3c), (2.3d, (2.3e), (2.3f), and (2.3g) yield:

$$(\mu_1+\gamma_1+\xi_1)I_1^n + \frac{dI_1}{dt} + h(\mu_1+\gamma_1+\xi_1)\frac{dI_1}{dt} + \left(\frac{h}{2!}\frac{d^2I_1}{dt^2} + \frac{h^2}{3!}\frac{d^3I_1}{dt^3} + \cdots\right)(1+h(\mu_1+\gamma_1+\xi_1)) = \phi_1 E_1^n, \tag{6.10}$$

$$R_1^n\mu_1 + \frac{dR_1}{dt} + h\mu_1\frac{dR_1}{dt} + \left(\frac{h}{2!}\frac{d^2R_1}{dt^2} + \frac{h^2}{3!}\frac{d^3R_1}{dt^3} + \cdots\right)(1+h\mu_1) = \gamma_1 I_1^n, \tag{6.11}$$

$$b\beta_2 I_1^n S_2^n + \mu_2 S_2^n + \frac{dS_2}{dt} + \left(\frac{h}{2!}\frac{d^2S_2}{dt^2} + \frac{h^2}{3!}\frac{d^3S_2}{dt^3} + \cdots\right)(1+hb\beta_2 I_1^n + h\mu_2) = \eta, \tag{6.12}$$

$$E_2^n(\theta_2+\mu_2) + \frac{dE_2}{dt} + h(\theta_2+\mu_2)\frac{dE_2}{dt} + \left(\frac{h}{2!}\frac{d^2E_2}{dt^2} + \frac{h^2}{3!}\frac{d^3E_2}{dt^3} + \cdots\right)(1+h(\theta_2+\mu_2)) = b\beta_2 I_1^n S_2^n, \tag{6.13}$$

$$I_2^n\mu_2 + \frac{dI_2}{dt} + h\mu_2\frac{dI_2}{dt} + \left(\frac{h}{2!}\frac{d^2I_2}{dt^2} + \frac{h^2}{3!}\frac{d^3I_2}{dt^3} + \cdots\right)(1+h\mu_2) = \theta_2 E_2^n. \tag{6.14}$$

Taking $h \to 0$, we obtain:

$$\frac{dI_1}{dt} = \phi_1 E_1^n - (\mu_1+\gamma_1+\xi_1)I_1^n, \tag{6.15}$$

$$\frac{dR_1}{dt} = \gamma_1 I_1^n - \mu_1 R_1^n, \tag{6.16}$$

$$\frac{dS_2}{dt} = \eta - b\beta_2 I_1^n S_2^n - \mu_2 S_2^n, \tag{6.17}$$

$$\frac{dE_2}{dt} = b\beta_2 I_1^n S_2^n - (\theta_2+\mu_2)E_2^n, \tag{6.18}$$

$$\frac{dI_2}{dt} = \theta_2 E_2^n - \mu_2 I_2^n. \tag{6.19}$$

Therefore, the NSFD method aligns with the system's behavior and hence, is consistent with the model.

6.3. **Numerical Results.** This section presents the numerical results of the system (2.3b)-(2.3g) using both the RK4 schemes from Equations (6.1a)-(6.1g) and the NSFD method from Equations (6.2a)-(6.2g). The results were generated using MATLAB with the following initial conditions at $t = 0$: for the human population, the susceptible individuals $S_1 = 55784$, exposed $E_1 = 250$, infected $I_1 = 216$, and recovered $R_1 = 0$. For the mosquito population, the susceptible individuals $S_2 = 168000$, exposed $E_2 = 10$, and infected $I_2 = 5$. The time delay factor was not applied in the first three cases. The behavior of solutions from RK4 and NSFD methods are investigated. Then, the time delay factor was applied for cases 4 and 5. In addition to the behavior of the numerical solutions, the classes and reproductive behavior are also analyzed.

Case 1: The graphs of the human and mosquito populations are displayed in Figures 7–10, respectively. These figures illustrate the graphical outputs of the SEIR-SEI system at DFE and EE points using the model's initial data. These results show that the system tends toward the DFE and EE points, ε_0 and ε_1, respectively. This behavior

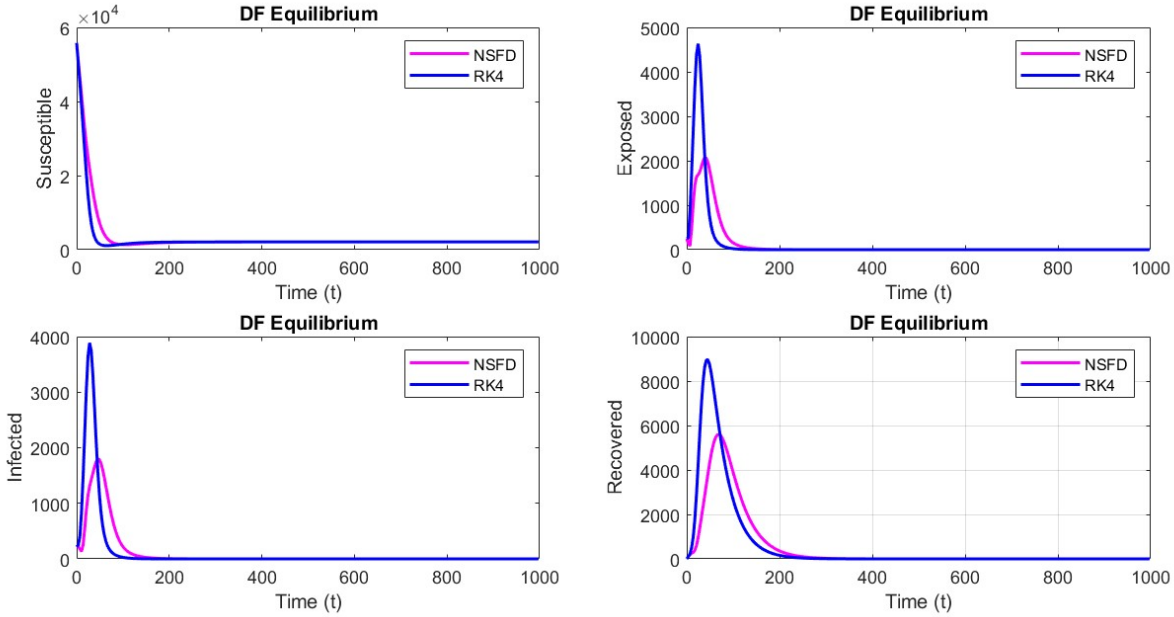

FIGURE 7. Human population, $h = 3.5$.

indicates stabilization at an endemic state. The basic reproduction number is $R_0 = 0.4868 < 1$ while in an endemic state, it is $R_0 = 3.3255 > 1$. These figures also reflect the combined effects of various model components, confirming the model's ability to capture key aspects of dengue fever transmission in both populations.

Case 2: Initially, both numerical schemes were evaluated with step size $h = 3.5$, where they successfully converged to the steady states ε_0 and ε_1, corresponding to the DFE and EE points, respectively. The solutions remain positive and bounded within the basic feasible region, indicating numerical stability and consistency with the continuous model. Furthermore, when the step size was set to $h = 5.5$, the graphs continues to show that the system dynamics tend toward the DFE point ε_0. However, the behavior changes for ε_1. The basic reproduction number $R_0 = 0.4868$ remains less than one for disease-free and 3.3255 for endemic which is greater than one. The RK4 and NSFD results remain accurate for disease-free points. For endemic points, RK4 method generated divergent results whereas the NSFD method convergent towards the steady states. The trajectories are displayed in Figures 11-14.

Case 3: In contrast, when the step size is increased to $h = 8$, with the system initialized near the DFE and EE points, a notable difference in the behavior of the numerical results was observed, as shown in Figures 15-18. The RK4 method fails to maintain stability and diverges from the expected solution, indicating sensitivity to larger step sizes. However, the NSFD method continues to produce a stable solution that converges toward the disease-free steady state. This supports the frequent use of the NSFD method in solving epidemiological models like dengue, malaria, and Rift Valley fevers [44]. This method ensures that the DFE and EE states are accurately captured, even under large time steps. These features are crucial when simulating long-term behavior in systems that involve disease transmission, control interventions, and population dynamics. The RK4 method, on the other hand, might require additional tuning (like adaptive step size control or error correction) to avoid numerical instabilities, which can be computationally expensive and less efficient.

Case 4: In this case, we undertake a comprehensive analysis of the impact of incorporating the endemic equilibrium into the mathematical model designed to study the dynamics of dengue fever transmission. The concept of endemic equilibrium refers to a state in which the disease persists in the population at a constant level over time, without either dying out or leading to widespread epidemic outbreaks. Including this equilibrium in the model allows us to examine the long-term behavior of the disease under realistic conditions and provides a more accurate representation of how

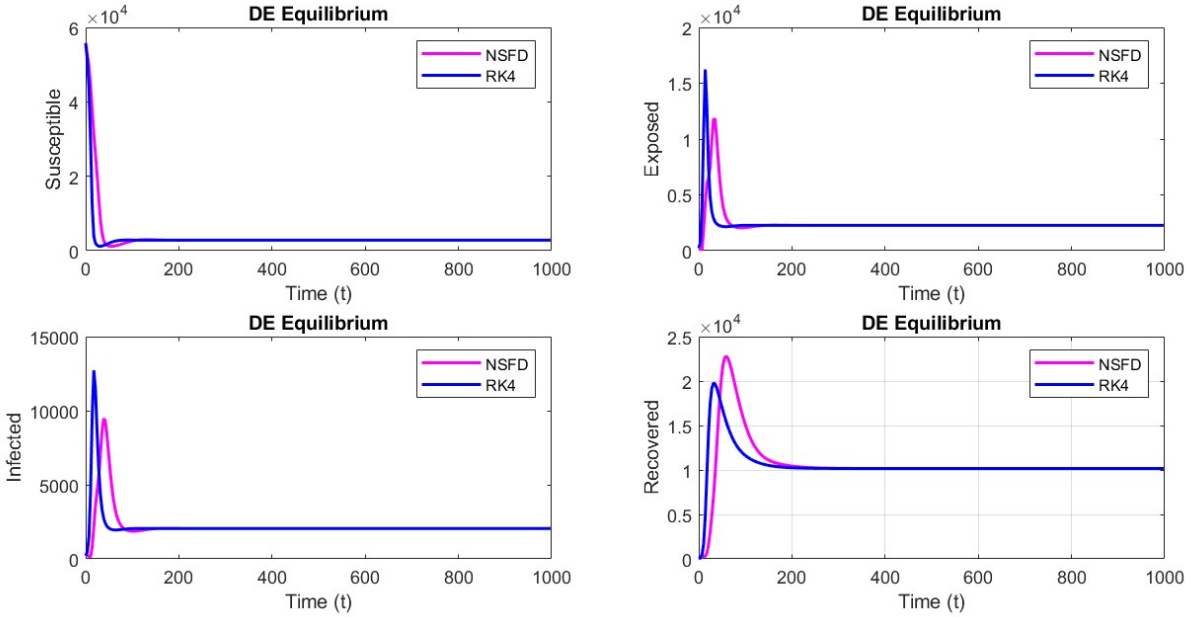

FIGURE 8. Human population, $h = 3.5$.

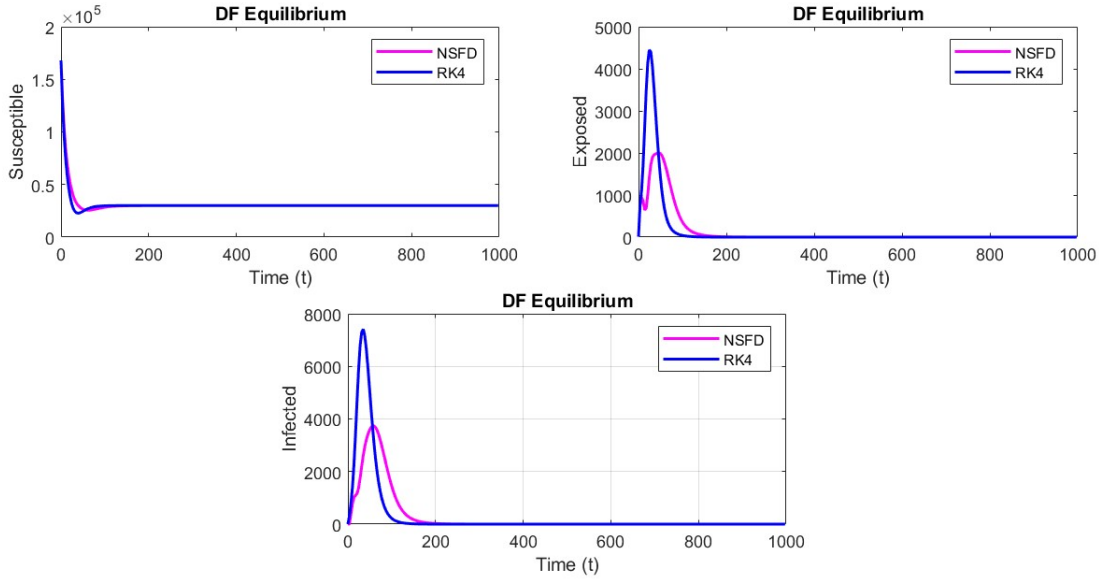

FIGURE 9. Mosquito population, $h = 3.5$.

dengue fever behaves in a population over extended periods. One of the critical parameters explored in this extended model is the time delay or exponential time delay, which represents the latency or delay between various biological or behavioral processes for instance, the delay between infection and the onset of symptoms, or the delay in implementing

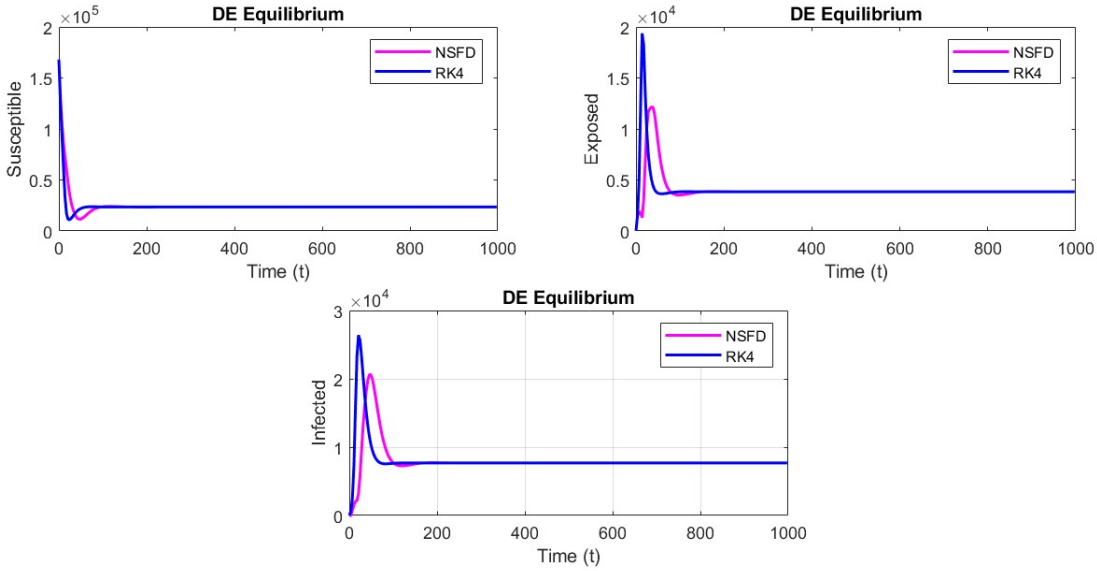

FIGURE 10. Mosquito population, $h = 3.5$.

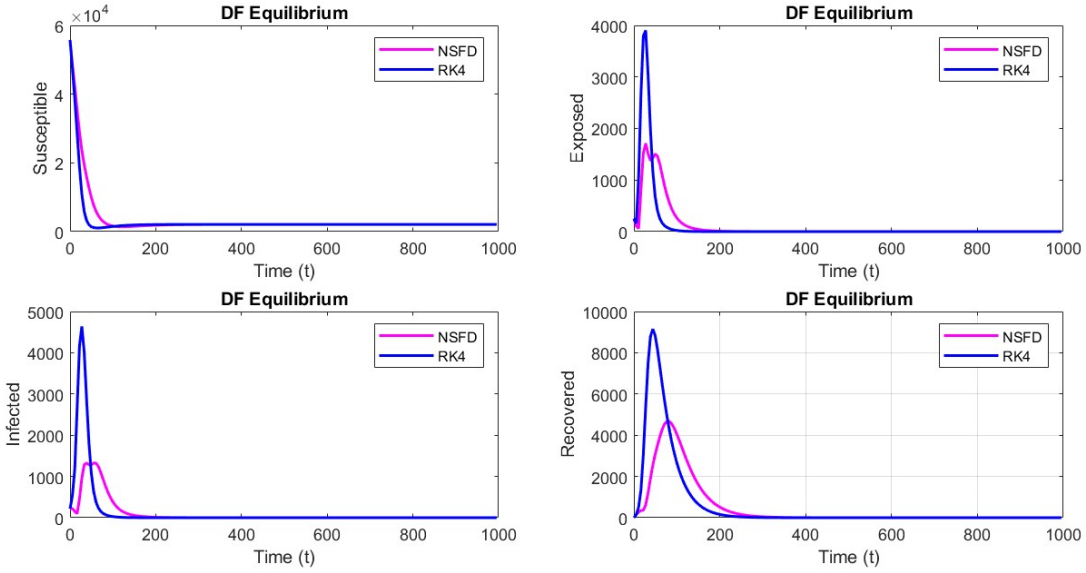

FIGURE 11. Human population, $h = 5.5$.

control measures after identifying cases. Our analysis reveals that this delay plays a pivotal role in shaping the overall trajectory of the disease. As shown in Figure 19, when time-delay strategies are introduced into the system either through delayed treatment, postponed vector control, or incubation periods there is a marked increase in the vulnerability of the human population to infection. This heightened vulnerability implies that susceptible individuals are at a greater risk of contracting the disease, possibly due to prolonged exposure or the inefficiency of delayed

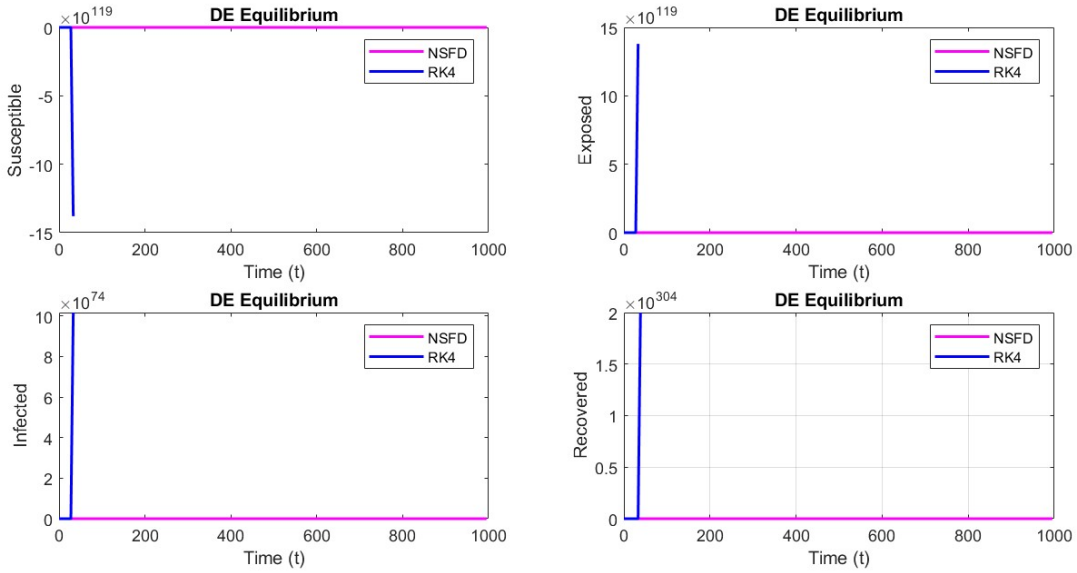

FIGURE 12. Human population, $h = 5.5$.

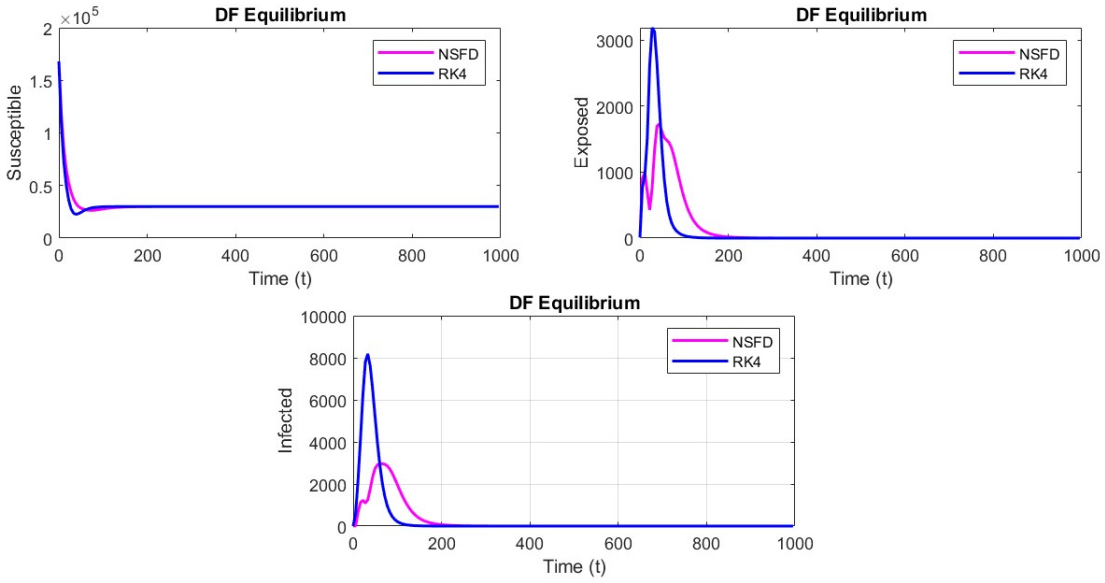

FIGURE 13. Mosquito population, $h = 5.5$.

responses in curbing transmission. However, an interesting counter-effect is observed in the infectivity of individuals who are already infected with dengue fever. With the implementation of time-delay mechanisms, the infectiousness of these individuals tends to decrease over time. This may be attributed to delayed isolation, treatment, or natural disease progression that limits the period during which an individual can transmit the virus. In certain scenarios, this infectivity can reduce so significantly that it nearly approaches zero, indicating that the individual's potential

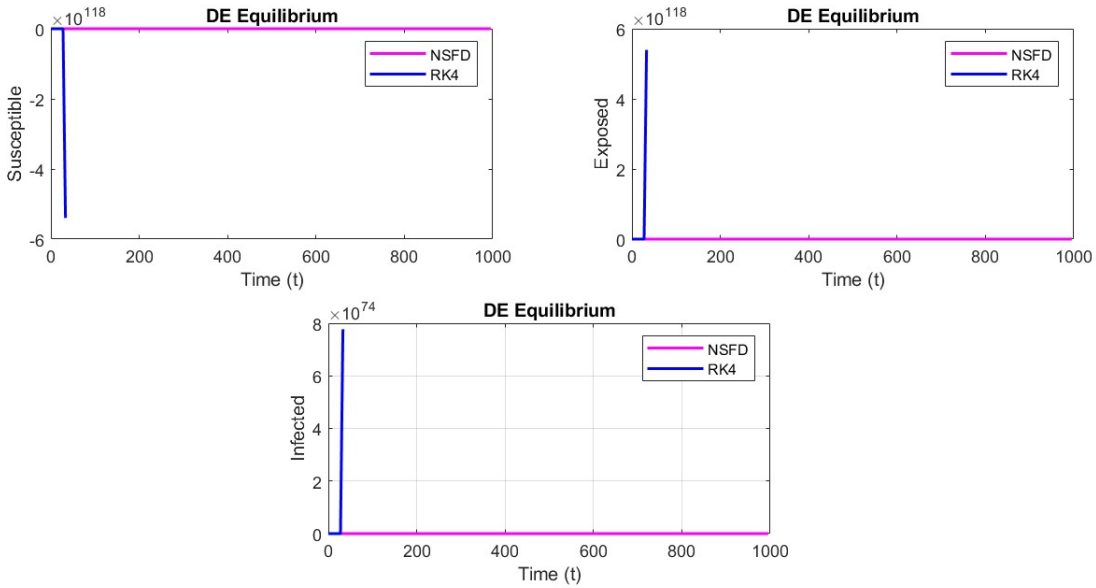

FIGURE 14. Mosquito population, $h = 5.5$.

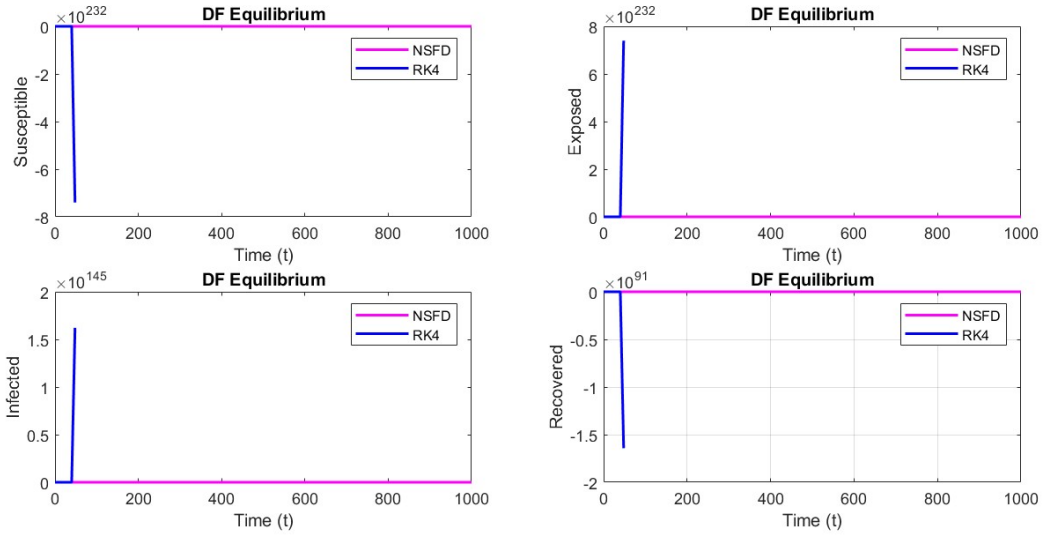

FIGURE 15. Human population, $h = 8$.

to spread the disease becomes negligible. This dual behavior where susceptibility increases but infectivity decreases suggests a complex interplay between time-dependent factors and disease dynamics. It highlights the importance of precisely timed intervention strategies, such as timely diagnosis, early treatment, and immediate vector control, in order to manage and potentially suppress the spread of dengue fever effectively. Thus, the incorporation of the endemic equilibrium and time delay into the model not only enriches our understanding of the disease's behavior but also underscores the need for time-sensitive public health policies to mitigate its impact.

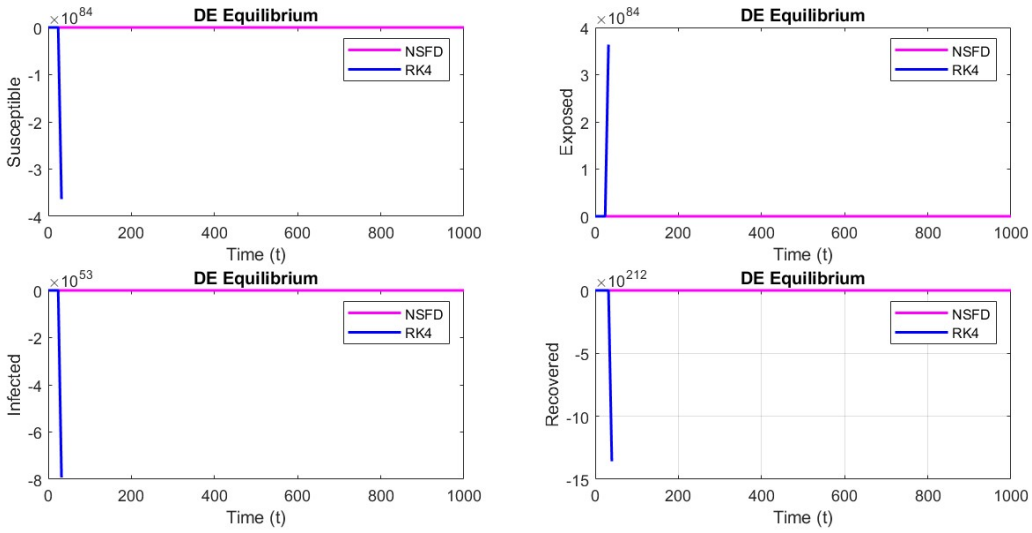

FIGURE 16. Human population, $h = 8$.

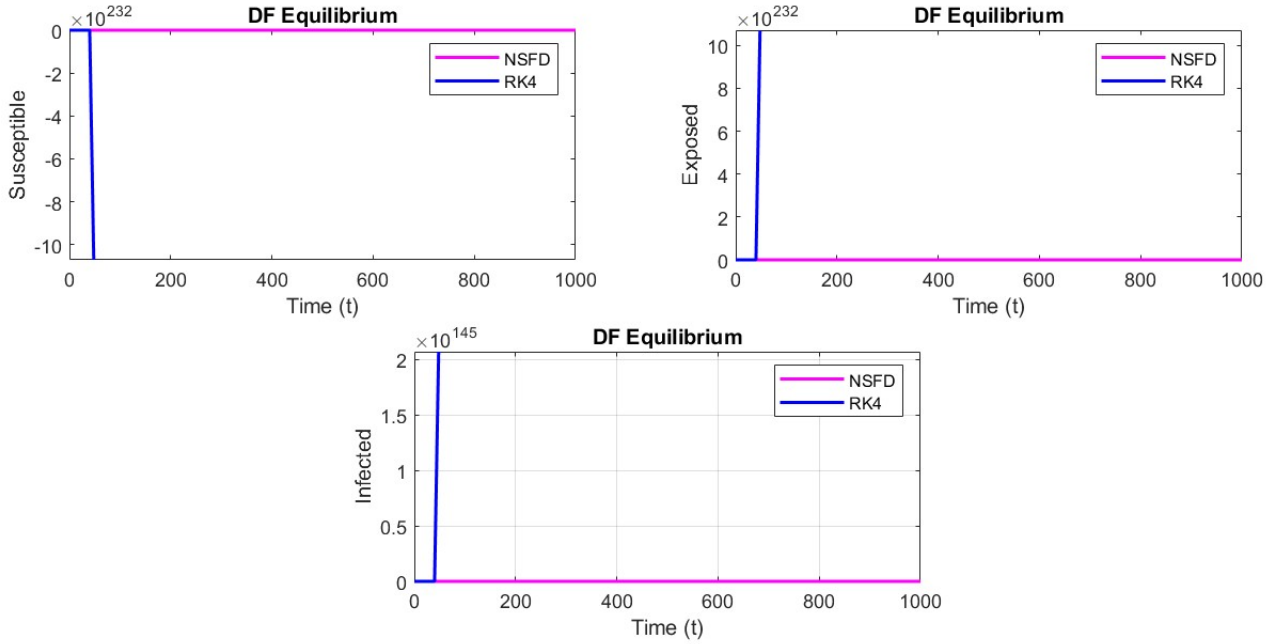

FIGURE 17. Mosquito population, $h = 8$.

Case 5: The comparison graph of the reproduction number and the chosen delay term (awareness, mosquito repellent and any government imposed factor) in Figure 20 illustrates that increasing the delay strategy effectively helps control the spread of dengue fever.

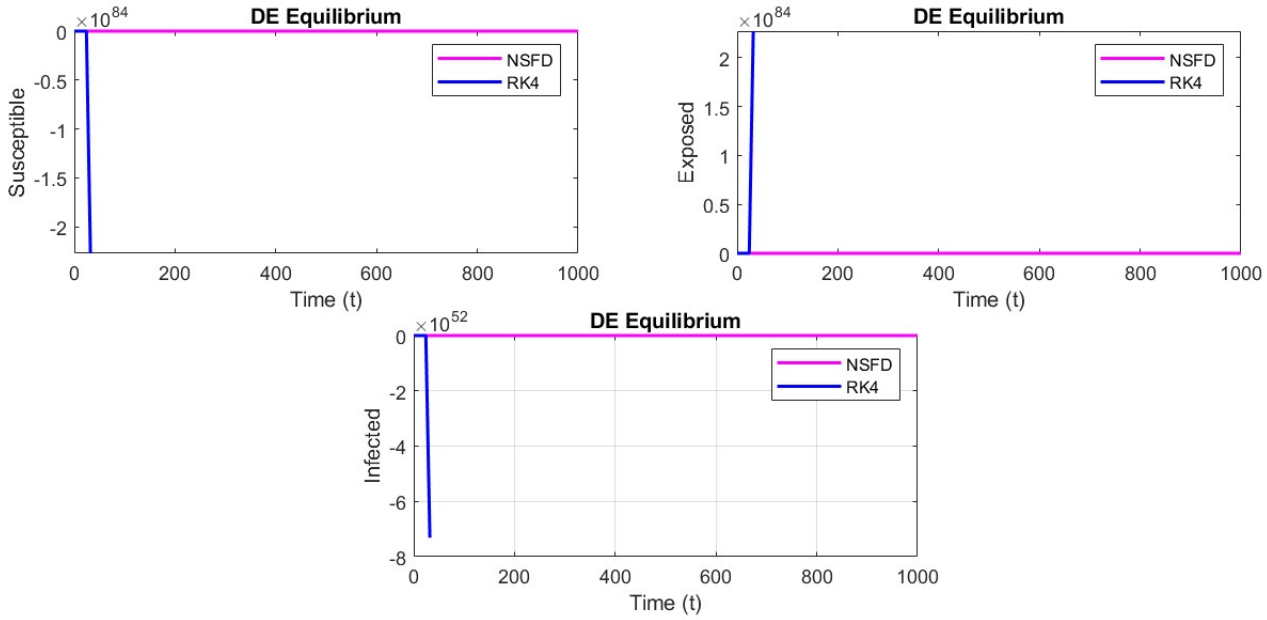

FIGURE 18. Mosquito population, $h = 8$.

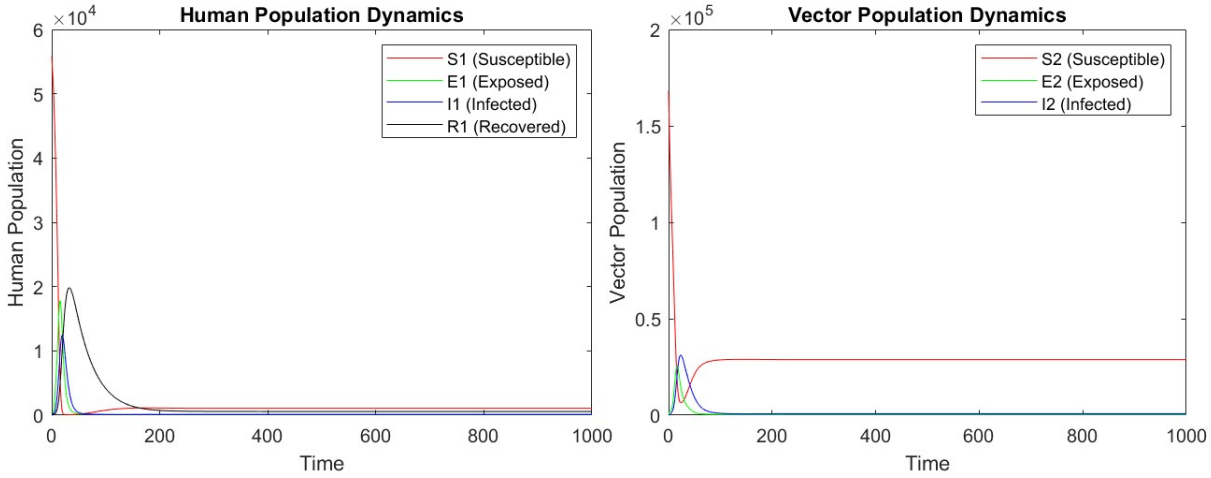

FIGURE 19. Combined behavior of the system with delay measure.

Hence, from the numerical results of different investigations, it is clear that we applied different mathematical methods to understand the influence of delay strategic planning in affecting the behavior of the SIER-SEI model. All in all, the numerical simulations highlight the effectiveness of the proposed SEIR-SEI model under varying conditions. While RK4 performs well for smaller step sizes, it becomes unstable for the larger ones. However, the NSFD method remains robust and reliable throughout [3, 4, 11, 32, 33, 37]. These results emphasize the importance of choosing appropriate numerical schemes for accurate disease modeling. The NSFD method proves to be a valuable tool in simulating the long-term dynamics of dengue transmission.

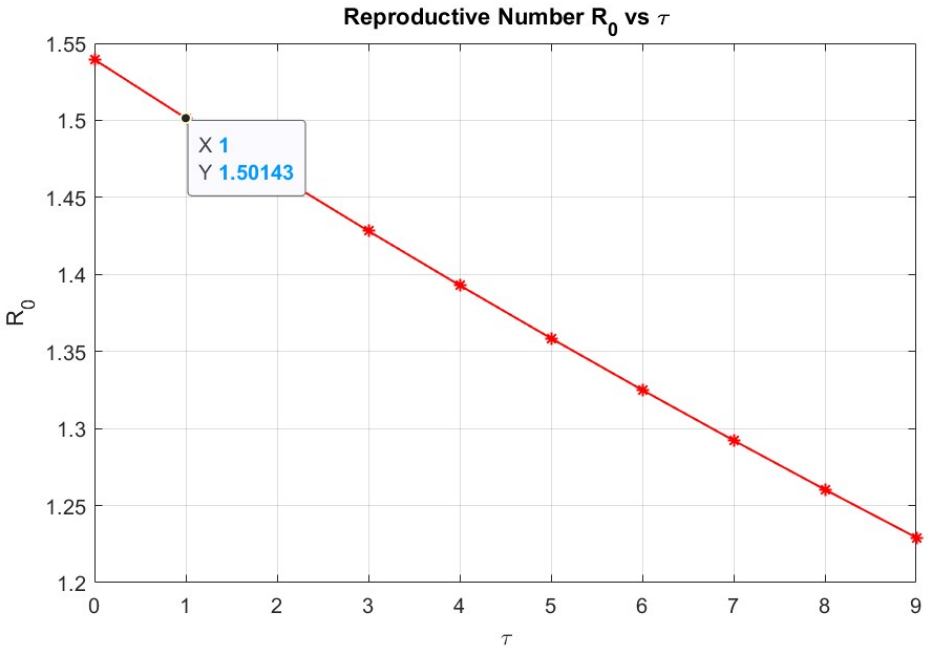

FIGURE 20. Comparison graph of the basic reproduction number and time delay term of the model.

7. Conclusion

In recent years, vector control and immunological strategies have emerged as promising approaches for dengue prevention and treatment all over the world. By targeting factors such as Wolbachia-infected mosquitoes and enhancing the host immune response, researchers aim to reduce dengue virus transmission and severity. However, individual and regional responses have varied significantly, and much remains unknown about the underlying biological and environmental causes. Moreover, conventional strategies that focus heavily on mosquito eradication may pose ecological risks, as mosquitoes contribute to biodiversity by serving as pollinators and a food source for other species. Recognizing these ecological implications, our study proposes a more balanced approach by emphasizing human-centered interventions. Specifically, we incorporate a delay factor in the human population to reflect real-world phenomena such as delayed awareness, diagnosis, or treatment. This choice was driven by the need for a dynamic, adaptive, and cost-efficient framework that balances disease reduction with resource constraints. This modeling choice offers a sustainable and ethically responsible framework for disease control, aligning public health goals with the preservation of ecological integrity. That is why in contrast to previous dengue modeling efforts, which predominantly employed classical SEIR with SIR framework without delay considerations, this study presents a novel SEIR-SEI model based on a system of DDEs incorporating delay factors. The inclusion of delay parameters reflecting incubation periods, treatment response time, and vector development provides a more realistic and robust framework for understanding dengue transmission. The innovative aspect of our research lies in utilizing numerical approaches for the DDE system. This work significantly contributes to a deeper understanding of the complex spatiotemporal dynamics of dengue transmission and the stability of key attractors (e.g., DFE and EE) under various realistic conditions.

The developed model incorporates four distinct subpopulations for humans: susceptible, exposed, infected, and recovered individuals, and three for vectors: susceptible, exposed, and infected. The analysis focuses on critical aspects such as the threshold parameter, equilibrium points, and positivity of the model. Additionally, the sensitivity of model parameters is thoroughly discussed. By performing a comprehensive sensitivity analysis, some key parameters such as transmission rates, delay periods, and other factors that significantly influence the basic reproduction number and the disease dynamics are identified. The most sensitive parameter involved is the biting rate b, the recruitment

rate of the human or host population Λ, and the transmission rate β_1. Therefore, we can reduce diseases by the time delay factor τ. It is indeed vital to equip and engage individuals who can serve as advocates and actively raise public awareness. These trained individuals will play a key role in motivating communities to adopt different strategies for lowering transmission rates. Promoting preventive actions such as wearing long-sleeved clothing, regularly applying mosquito repellent, and maintaining proper hygiene can significantly help in controlling the spread of dengue. Furthermore, awareness initiatives led by these advocates can inspire people to think innovatively and take proactive steps to further reduce the risk of transmission. These findings demonstrate that our model provides a more realistic representation of dengue transmission and serves as a powerful analytical tool for assessing intervention strategies. The model's structure allows for flexible integration of control measures like treatment, awareness campaigns, or Wolbachia mosquito deployment, making it particularly valuable for scenario-based simulations and public health planning. Therefore, this work contributes both theoretically and practically to the understanding and management of dengue in endemic regions.

Local stability is assessed using the Routh-Hurwitz and Jacobian criteria, while global stability is ensured through the LaSalle invariance principle and Lyapunov theory. Our findings demonstrate that the DFE is locally and globally asymptotically stable when the basic reproduction number is less than unity, whereas an EE emerges when it exceeds unity. Finally, we have applied the numerical schemes of RK4 and NSFD methods on the proposed model to acquire numerical solutions of the SEIR-SEI dengue delay transmission model. RK4 is not suitable for large step sizes but the NSFD method demonstrates superior stability, robustness, and adherence to biological bounds even over extended time intervals. The results reveal that the NSFD method is both stable and reliable. In modelling the spread of dengue, the NSFD method offers considerable advantages, particularly regarding accuracy, stability, and computational complexity. It is specifically designed to preserve essential properties of continuous systems, such as positivity and convergence, which are critical for biological epidemic models. To complement the theoretical analysis of the dengue transmission model, we employed the RK4 and NSFD methods not merely as numerical solvers, but as validation frameworks for model fidelity. The RK4 method provided highly accurate time-step predictions suitable for short-term forecasting, while the NSFD scheme preserved the model's biological consistency and positivity of solutions, even under larger step sizes. Their combined use demonstrated that the mathematical integrity of the model is maintained across different numerical regimes. This hybrid approach strengthens the model's applicability to real-world policy simulations, where precision and structure preservation are both critical. Therefore, the inclusion of RK4 and NSFD serves not as a redundancy, but as a strategic bridge between theoretical rigor and computational practicality. Overall, the NSFD method is preferred for long-term integration of epidemic models as it maintains the qualitative dynamics of the system. These findings are relevant globally, where public attitude, government support, and environmental conditions play a critical role in dengue transmission. By incorporating these socio-environmental factors into the mathematical model, we propose a flexible and context-aware modeling framework suitable for varying public health landscapes and regional dynamics. Furthermore, this model can be extended globally, enabling other dengue-endemic countries to tailor control strategies based on local perceptions, environmental dynamics, and healthcare infrastructure. The future directions include stochastic, fractional, and fuzzy extensions of the current work.

Acknowledgment

We gratefully acknowledge the financial support provided by Universiti Sains Malaysia (Main Campus) and the Malaysian International Scholarship. We also extend our sincere gratitude to the reviewers and the editorial team of the Computational Methods for Differential Equations (CMDE) for their insightful comments and constructive feedback, which significantly enhanced the quality of this work.

Use of AI tools declaration and Data availability

The authors declare they have not used Artificial Intelligence (AI) tools in the creation of this article. However, for rephrasing ChatGpt and Quiltbolt were used. Also, All data is available inside the article.

Conflict of interest

The authors declare no conflicts of interest.

References

[1] A. Abidemi and N. A. B. Aziz, *Analysis of deterministic models for dengue disease transmission dynamics with vaccination perspective in Johor, Malaysia*, International Journal of Applied and Computational Mathematics, *8*(1) (2022), 45.

[2] S. AbuBakar, S. E. W. Puteh, R. Kastner, L. Oliver, S. H. Lim, R. Hanley, and E. Gallagher, *Epidemiology (2012-2019) and costs (2009-2019) of dengue in Malaysia: a systematic literature review*, International Journal of Infectious Diseases, *124* (2022), 240-247.

[3] W. Ahmad, A. I. K. Butt, N. Akhtar, M. Rafiq, M. Gohar, Z. Idrees, and N. Ahmad, *Developing computationally efficient optimal control strategies to eradicate Rubella disease*, Physica Scripta, *99*(3) (2024), 035202.

[4] W. Ahmad, M. Rafiq, A. I. K. Butt, N. Ahmad, T. Ismaeel, S. Malik, H. G. Rabbani, and Z. Asif, *Analytical and numerical explorations of optimal control techniques for the bi-modal dynamics of Covid-19*, Nonlinear Dynamics, *112*(5) (2024), 3977-4006.

[5] K. A. Aldwoah, M. A. Almalahi, K. Shah, M. Awadalla, and R. H. Egami, *Dynamics analysis of dengue fever model with harmonic mean type under fractal-fractional derivative*, AIMS Mathematics, *9*(6) (2024), 13894-13926.

[6] T. D. Alharbi and M. R. Hasan, *Global stability and sensitivity analysis of vector-host dengue mathematical model*, AIMS Mathematics, *9*(11) (2024), 32797-32818.

[7] R. K. Alhefthi, M. A. ur Rehman, N. Ahmed, Z. Iqbal, M. Inc, M. Iqbal, M. S. Iqbal, A. Raza, and M. Rafiq, *Developing a computational framework for accurately solving a mathematical model of Streptococcus pneumonia infection*, Biomedical Signal Processing and Control, *103* (2025), 107427.

[8] S. A. Bakar and N. Shafee, *Outlook of dengue in Malaysia: a century later*, Malaysian Journal of Pathology, *24*(1) (2002), 23-27.

[9] S. Bhatter, B. Bhatia, S. Kumawat, and S. Purohit, *Modeling and simulation of COVID-19 disease dynamics via Caputo Fabrizio fractional derivative*, Computational Methods for Differential Equations, *Online First* (2024).

[10] O. Brathwaite Dick, J. L. San Martín, R. H. Montoya, J. del Diego, B. Zambrano, and G. H. Dayan, *The history of dengue outbreaks in the Americas*, The American journal of tropical medicine and hygiene, *87*(4) (2012), 584-593.

[11] A. I. K. Butt, W. Ahmad, M. Rafiq, N. Ahmad, and M. Imran, *Computationally efficient optimal control analysis for the mathematical model of Coronavirus pandemic*, Expert Systems with Applications, *234* (2023), 121094.

[12] H. Dieng, R. G. Saifur, A. H. Ahmad, M. C. Salmah, A. T. Aziz, T. Satho, F. Miake, Z. Jaal, S. Abubakar, and R. E. Morales, *Unusual developing sites of dengue vectors and potential epidemiological implications*, Asian Pacific Journal of Tropical Biomedicine, *2*(3) (2012), 228-232.

[13] Y. Dumont and J. Thuilliez, *Human behaviors: A threat to mosquito control?*, Mathematical Biosciences, *281* (2016), 9-23.

[14] C. Dye, *Vectorial capacity: Must we measure all its components?*, Parasitology Today, *2*(8) (1986), 203-209.

[15] E. L. Fairbanks, M. Saeung, A. Pongsiri, E. Vajda, Y. Wang, D. J. McIver, J. H. Richardson, A. Tatarsky, N. F. Lobo, S. J. Moore, A. Ponlawat, T. Chareonviriyaphap, A. Ross, and N. Chitnis, *Inference for entomological semi-field experiments: Fitting a mathematical model assessing personal and community protection of vector-control interventions*, Computers in Biology and Medicine, *168* (2024), 107716.

[16] H. Gholami, M. Gachpazan, and M. Erfanian, *SEIaIsQRS epidemic model for COVID-19 by using compartmental analysis and numerical simulation*, Computational Methods for Differential Equations, *Online First* (2024).

[17] K. Gosztonyi, *How history of mathematics can help to face a crisis situation: the case of the polemic between Bernoulli and d'Alembert about the smallpox epidemic*, Educational Studies in Mathematics, *108*(1-2) (2021), 105-122.

[18] N. Hamdan Izzati and A. Kilicman, *Local stability of dengue model using the fractional order system with different memory effect on the host and vector population*, Thermal Science, *23*(Suppl. 1) (2019), 327-337.

[19] N. Hamdan Izzati and A. Kilicman, *Analysis of the fractional order dengue transmission model: a case study in Malaysia*, Advances in Difference Equations, *2019*(1) (2019).

[20] N. Hamdan Izzati and A. Kilicman, *The development of a deterministic dengue epidemic model with the influence of temperature: A case study in Malaysia*, Applied Mathematical Modelling, *90* (2021), 547-567.

[21] H. Hassan, S. Shohaimi, and N. R. Hashim, *Risk mapping of dengue in Selangor and Kuala Lumpur, Malaysia*, Geospatial Health, *7*(1) (2012), 21.
[22] W. O. Kermack and A. G. McKendrick, *Contributions to the mathematical theory of epidemics-I*, Bulletin of Mathematical Biology, *53*(1-2) (1991), 33-55.
[23] M. B. Khan, Z. S. Yang, C. Y. Lin, M. C. Hsu, A. N. Urbina, W. Assavalapsakul, W. H. Wang, Y. H. Chen, and S. F. Wang, *Dengue overview: An updated systemic review*, Journal of Infection and Public Health, *16*(10) (2023), 1625-1642.
[24] J. L. Kyle and E. Harris, *Global spread and persistence of dengue*, Annual Review of Microbiology, *62*(1) (2008), 71-92.
[25] S. Mandal, R. R. Sarkar, and S. Sinha, *Mathematical models of malaria-a review*, Malaria journal, *10* (2011), 1-19.
[26] S. B. Mohamed Siddik, F. A. Abdullah, and A. I. Md. Ismail, *Mathematical model of dengue virus with predator-prey interactions*, Sains Malaysiana, *49*(5) (2020), 1191–1200.
[27] S. N. Mohd Salleh, N. Che Dom, S. Ab Rahim, E. Mohamed, N. Haron, A. S. Rambely, and S. N. Camalxaman, *Dengue vector control approaches: existing options and the way forward*, Journal Of Sustainability Science And Management, *17*(12) (2022), 227-238.
[28] A. H. Mohd-Zaki, J. Brett, E. Ismail, and M. L'Azou, *Epidemiology of dengue disease in Malaysia (2000–2012): a systematic literature review*, PLoS Neglected Tropical Diseases, *8*(11) (2014), e3159.
[29] M. R. Mohd Abd Razak, N. Mohmad Misnan, N. H. Md Jelas, N. A. Norahmad, A. Muhammad, T. C. D. Ho, B. Jusoh, U. R. Sastu, M. Zainol, M. I. Wasiman, H. Muhammad, R. Thayan, and A. F. Syed Mohamed, *The effect of freeze-dried Carica papaya leaf juice treatment on NS1 and viremia levels in dengue fever mice model*, BMC Complementary and Alternative Medicine, *18*(1) (2018).
[30] K. Mulligan, S. J. Elliott, and C. Schuster-Wallace, *The place of health and the health of place: Dengue fever and urban governance in Putrajaya, Malaysia*, Health & Place, *18*(3) (2012), 613-620.
[31] N. E. A. Murray, M. B. Quam, and A. Wilder-Smith, *Epidemiology of dengue: past, present and future prospects*, Clinical Epidemiology, *5* (2013), 299-309.
[32] M. Naveed, D. Baleanu, M. Rafiq, A. Raza, A. H. Soori, and N. Ahmed, *Dynamical behavior and sensitivity analysis of a delayed coronavirus epidemic model*, Computers Materials & Continua, *65*(1) (2020), 225-241.
[33] M. Naveed, M. Rafiq, A. Raza, N. Ahmed, I. Khan, K. Sooppy Nisar, and A. Hassan Soori, *Mathematical analysis of novel Coronavirus (2019-nCov) delay pandemic model*, Computers Materials & Continua, *64*(3) (2020), 1401–1414.
[34] E. L. Pang and H. S. Loh, *Current perspectives on dengue episode in Malaysia*, Asian Pacific Journal of Tropical Medicine, *9*(4) (2016), 395-401.
[35] H. J. Peng, H. B. Lai, Q. L. Zhang, B. Y. Xu, H. Zhang, W. H. Liu, W. Zhao, Y. P. Zhou, X. G. Zhong, S. Jiang, J. H. Duan, G. Y. Yan, J. F. He, and X. G. Chen, *A local outbreak of dengue caused by an imported case in Dongguan, China*, BMC Public Health, *12*(1) (2012), 83.
[36] R. Prem Kumar, G. S. Mahapatra, S. Basu, and P. K. Santra, *Global stability and sensitivity analysis of dengue transmission using four host and three vector classes along with control strategies*, International Journal of Computer Mathematics, *1* (2024), 1-26.
[37] A. Raza, A. Ahmadian, M. Rafiq, S. Salahshour, M. Naveed, M. Ferrara, and A. H. Soori, *Modeling the effect of delay strategy on transmission dynamics of HIV/AIDS disease*, Advances in Difference Equations, *2020*(1) (2020), 663.
[38] A. Raza, K. Ali, S. T. R. Rizvi, S. Sattar, and A. R. Seadawy, *Discussion on vector control dengue epidemic model for stability analysis and numerical simulations*, Brazilian Journal of Physics, *55*(1) (2024).
[39] A. Singh and A. W. Taylor-Robinson, *Vector control interventions to prevent dengue: current situation and strategies for future improvements to management of Aedes in India*, Journal of Infectious Disease and Pathology, *2*(1) (2017), 1-8.
[40] C. J. Tay, M. Fakhruddin, I. S. Fauzi, S. Y. Teh, M. Syamsuddin, N. Nuraini, and E. Soewono, *Dengue epidemiological characteristic in Kuala Lumpur and Selangor, Malaysia*, Mathematics and Computers in Simulation, *194*

(2022), 489-504.
[41] P. Van Den Driessche, *Reproduction numbers of infectious disease models*, Infectious Disease Modelling, *2*(3) (2017), 288-303.
[42] World Health Organization, *Dengue and severe dengue*, World Health Organization, (2021). Available at: https://www.who.int/westernpacific/emergencies/surveillance/dengue.
[43] L. P. Wong, S. M. M. Shakir, N. Atefi, and S. AbuBakar, *Factors affecting dengue prevention practices: Nationwide survey of the Malaysian public*, PLOS ONE, *10*(4) (2015), e0122890.
[44] S. Zeb, S. A. Mohd Yatim, M. Rafiq, W. Ahmad, A. Kamran, and M. F. Karim, *Treatment and delay control strategy for a non-linear rift valley fever epidemic model*, AIP Advances, *14*(11) (2024).
[45] S. Zeb, S. A. Mohd Yatim, A. Ahmad, A. Kamran, and M. Rafiq, *Numerical modelling of SEIR on two-dose vaccination against the rubella virus*, Malaysian Journal of Fundamental and Applied Sciences, *21*(1) (2025), 1577-1601.
[46] S. Zeb, S. A. Mohd Yatim, S. Lal, A. Kamran, A. Ahmad, and M. Rafiq, *Numerical analysis of the NSP epidemic model for campus drinking dynamics*, Semarak International Journal of Fundamental and Applied Mathematics, *4*(1) (2024), 48–60.